

Dual Band Circularly Polarized Proximity Coupled Stacked Patch Antenna for RF Energy Harvesting



By

Samra Khalid

00000326155

MSEE-RF&MW-2020

Supervisor

Dr. Mohaira Ahmad

Department of Electrical Engineering

School of Electrical Engineering and Computer Science (SEECS)


National University of Sciences and Technology (NUST),

Islamabad, Pakistan.

Dec 2023


Thesis acceptance certificate

Certified that final copy of MS/MPhil thesis written by Miss Samra Khalid, Registration No. 00000326155 of SEECs (School/College/Institute) has been vetted by undersigned, found complete in all respects as per NUST Statutes/Regulations, is free of plagiarism, error and mistakes and is accepted as partial fulfillment for award of MS/MPhil degree. It is further certified that necessary amendments as pointed out by GEC members of the scholar have also been incorporated in the said thesis.

Signature:  _____

Name of Supervisor: Dr. Mohaira Ahmad

15-01-2024

Signature (HOD):  _____

Date: 15-01-2024

Signature (Dean/Principal):  _____

Date: 23 Jan, 2024

Approval

It is certified that the contents and form of the thesis entitled “Dual Band Circularly Polarized Proximity Coupled Stacked Patch Antenna for RF Energy Harvesting” submitted by “Samra Khalid” have been found satisfactory for the requirement of the degree.

Advisor: Dr. Mohaira Ahmad

Signature:



Date:

15-1-2024

Committee Member 1:

Dr. Noshawan Shoaib

Signature:



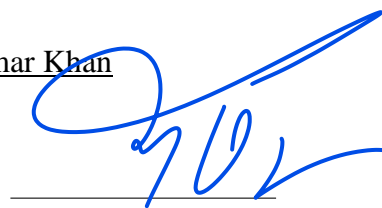
Date:

23-01-2024

Committee Member 2:

^{M.}
Dr. Umar Khan

Signature:



Date:

23-1-24

Dedication

I dedicate this research to my fellow researchers and my parents who have always supported me in my dreams. My siblings and my friends who have been a massive force throughout this journey. Lastly, I want to dedicate this thesis to my supervisor Dr. Mohaira Ahmed who has helped me in every step of this meaningful learning process.

Certificate of Originality

I hereby declare that this submission is my own work and to the best of my knowledge it contains no materials previously published or written by another person, nor material which to a substantial extent has been accepted for the award of any degree or diploma at SEECS NUST or at any other educational institute, except where due acknowledgement has been made in the thesis. Any contribution made to the research by others, with whom I have worked at SEECS NUST or elsewhere, is explicitly acknowledged in the thesis.

I also declare that the intellectual content of this thesis is the product of my own work, except for the assistance from others in the project's design and conception or in style, presentation and linguistics which has been acknowledged.

Author Name: Samra Khalid

Registration No. 00000326155

Signature: Samra

Acknowledgements

First of all, I am very thankful to almighty ALLAH the most merciful and the most beneficent who gave me the strength, wisdom and enlightened me to complete this research work.

I am grateful to my thesis advisor, Dr. Mohaira Ahmed, for supervising my work. The door to her office was always open whenever I needed some help in my research or writing. Her constant support and guidance made it possible for me to complete my thesis.

I would also like to express my deepest gratitude to my parents for their support throughout my life. I am also thankful to Mr. Fahad Khalid for his assistance in performing the measurements. I would also like to acknowledge my seniors at SEECS, especially Mr. Ali Anjum for a valuable discussion on proximity coupled feeding.

I am also very grateful to my committee members, Dr. Umar Khan, and Dr. Noshewan Shoaib, for their valuable input.

Contents

Table of Contents

Acknowledgements	vi
List of Figures	xi
Abstract	xiv
Introduction	1
1.1. Antennas	1
1.2. Types of Antennas	2
1.2.1. Wire Antennas	3
1.2.2. Aperture Antennas	3
1.2.3. Microstrip Antennas	4
1.2.4. Array Antennas.....	5
1.2.5. Reflector Antennas	5
1.2.6. Lens Antennas	6
1.3. Antenna Radiation Pattern.....	7
1.3.1. Field Pattern.....	7
1.3.2. Power Pattern (Linear Scale)	7
1.3.3. Power Pattern (dB Scale)	7
1.4. Radiation Pattern Lobes	8
1.4.1. Major Lobe	8
1.4.2. Minor Lobe	8
1.4.3. Side Lobe.....	8
1.4.4. Back Lobe.....	8

1.5.	Radiation Power Density	8
1.6.	Radiation Intensity	8
1.7.	Beam width.....	9
1.8.	Directivity.....	9
1.9.	Beam Efficiency	10
1.10.	Bandwidth	10
1.11.	Gain	10
1.12.	Antenna Efficiency.....	10
1.13.	Input Impedance	11
1.14.	Polarization.....	11
1.14.1.	Linear Polarization.....	12
1.14.1.1.	Vertical Polarization	12
1.14.1.2.	Horizontal Polarization	12
1.14.2.	Slant Polarization.....	12
1.14.3.	Circular Polarization.....	13
1.14.4.	Elliptical Polarization	13
1.15.	Friis Equation of Transmission	13
1.16.	Feeding Methods	14
1.16.1.	Contacting Feeding Method.....	14
1.16.1.1.	Microstrip Feeding Method	14
1.16.1.2.	Coaxial Feeding Method.....	15
1.16.2.	Non Contacting Feeding Method.....	16
1.16.2.1.	Aperture Coupled Feeding Method	16
1.16.2.2.	Proximity Coupled Feeding Method.....	16
1.17.	RF Energy Harvesting	17

1.17.1. Incorporation with other technologies	18
1.18. Thesis Objectives	19
1.19. Advantages.....	19
1.20. Areas of Application.....	19
Chapter # 02	20
Literature Review.....	20
2.1. Background.....	20
2.2. Broadband Rectenna with Matching Network Elimination.....	21
2.3. Novel Broadband and Frequency Selective Rectennas for a Wide Input Power and Load Impedance	26
2.4. 3D Quad band Array Rectenna for Efficient Energy Harvesting	29
2.5. Planar 3D Rectenna Array for Wireless Power Transfer Sensor Nodes.....	32
2.6. Literature Review Table	36
Chapter # 3	38
Research Methodology.....	38
3.1 An impedance matching method for broadband proximity coupled microstrip antenna	38
3.1.1. Design	38
3.1.2. Result and Discussion	40
3.1.3. Conclusion.....	41
3.2. A Dual-polarized Broadband Cavity backed Proximity-coupled Microstrip Antenna	41
3.2.1. Design.....	41
3.2.2. Results and Discussions	42
3.2.3. Conclusion.....	44
3.3. Novel Broadband Proximity Coupled Microstrip Antenna Application for Conformal Phased Array Design.....	44

3.3.1. Design.....	45
3.3.2. Results and Discussions	46
3.3.3. Conclusion.....	47
3.4. Design of a antenna with a square backed cavity and dual polarization	47
3.4.1. Design.....	47
3.4.2. Results and Discussions	48
3.4.3. Conclusion.....	50
Chapter # 04	51
Dual Band CP Microstrip Patch Antenna for RF Energy Harvesting	51
4.1. Introduction.....	51
4.2 Design Evolution	52
4.2.1. Simulated Results:	53
4.3. Design Challenges	57
4.2.4. Circular Polarization	64
4.2.5. Fabricated Prototype	65
4.2.6. Measured Results.....	66
4.2.7. Radiation Patterns	68
4.2.7.1. Azimuth Plane.....	69
4.2.7.2. Elevation Plane	70
4.2.8. Results Comparison	71
Chapter # 5	73
Conclusion and Future Recommendations.....	73
5.1. Conclusion	73
5.2. Future Recommendations	74
REFERENCES	75

APPENDIX A	78
Abbreviations & Acronyms.....	78

List of Figures

Figure 1.1 Antenna as a transition device	2
Figure 1.2 Types of Antennas	2
Figure 1.3 Wire Antennas	3
Figure 1.4 Aperture Antennas	4
Figure 1.5 Microstrip Antennas	4
Figure 1.6 Antenna Arrays.....	5
Figure 1.7 Reflector Antenna Arrays.....	6
Figure 1.8 Horn Lens Antenna.....	6
Figure 1.9 Radiation Patterns in free space of periodic straight wire antenna	7
Figure 1.10 Beam width of an antenna	9
Figure 1.11 Classification of Polarization	12
Figure 1.12 Circular Polarization.....	13
Figure 1.13 Microstrip Fed Patch Antenna [1]	15
Figure 1.14 Coaxial fed patch antenna [1].....	15
Figure 1.15 Aperture coupled fed patch [1].....	16
Figure 1.16 Proximity fed patch antenna [1]	17
Figure 1.17 RF Energy Harvesting	18
Figure 1.18 Hybrid Energy harvesting system model with solar and RF energy	19
Figure 2.19 CST Design of the broadband antenna [14]	22
Figure 2.20 Broadband antenna results [14]	23
Figure 2.21 Simulated results of the broadband antenna	23
Figure 2.22 Antenna design for OCFD antenna [14].....	24
Figure 2.23 Offcentre-fed dipole antenna results [14].....	25
Figure 2.24 Simulated results for off-centre fed dipole antenna	26
Figure 2.25 Novel Broadband Frequency Selective Rectenna [15].....	27
Figure 2.26 CST Design of the novel broadband antenna	27
Figure 2.27 Novel Broadband FSS Rectenna results [15]	28
Figure 2.28 Simulated results of Novel Broadband Antenna	28
Figure 2.29 ADS design of the rectifier	29
Figure 2.30 Bowtie Antenna for energy harvesting [16]	30
Figure 2.31 CST Design of the Bowtie Antenna	30
Figure 2.32 Bowtie Antenna Results [16].....	31
Figure 2.33 CST Design results of the bowtie antenna	31

Figure 2.34 Radiation Patterns of the bowtie Antenna [16]	32
Figure 2.35 CST Design Radiation Pattern of bowtie antenna.....	32
Figure 2.36 3D Radial Rectenna Array for RF Energy Harvesting [20]	33
Figure 2.37 CST Design for (a) Bore sight Antenna (b) End fire Antenna.....	34
Figure 2.38 Return loss results for bore sight antenna and end fire antenna [20]	34
Figure 2.39 CST design results for bore sight and end fire antenna.....	35
Figure 2.40 Radiation Patterns for Bore sight and End fire Antenna [20]	35
Figure 3.41 Antenna configuration [21]	39
Figure 3.42 Geometry of the cavity [21]	39
Figure 3.43 VSWR of cavity backed antenna [21]	40
Figure 3.44 Antenna Input Impedance without cavity [21].....	40
Figure 45 Antenna Input Impedance with cavity [21]	41
Figure 3.46 Cavity backed antenna with side view and top view [22].....	42
Figure 3.47 Simulation and measured result of the antenna [22]	43
Figure 3.48 Simulated and Measured results of E-plane at 9.8GHz [22].....	43
Figure 3.49 Simulation and Measurement results of H-plane at 9.8GHz [22]	44
Figure 3.50 Structure of the proposed antenna [23]	45
Figure 3.51 Results of the proposed antenna [23]	46
Figure 3.52 Prototype conformal phased array antenna [23].....	46
Figure 3.53 DP microstrip patch antenna structure [24].....	48
Figure 3.54 DP microstrip patch antenna structure (complete view) [24].....	48
Figure 3.55 S11 plot for 1port [24].....	49
Figure 3.56 S11 plot for all four ports [24].....	49
Figure 3.57 Radiation pattern plot for one port [24].....	50
Figure 3.58 Radiation pattern for all four ports [24].....	50
Figure 4.59 Proximity Coupled Stacked Patch Antenna	52
Figure 4.60 S11 of the stacked microstrip patch antenna	53
Figure 4.61 Radiation Pattern at 1.8GHz.....	54
Figure 4.62 Radiation Pattern at 2.4GHz.....	54
Figure 4.63 3D Radiation Pattern at 1.8GHz (5880)	55
Figure 4.64 3D Radiation Pattern at 2.4GHz (5880)	55
Figure 4.65 Antenna Radiation Efficiency	56
Figure 4.66 Antenna Total Efficiency	57
Figure 4.67 S11 of the stacked microstrip patch antenna (substrate 5880)	58
Figure 4.68 Antenna Radiation Pattern at 1.8GHz	58
Figure 4.69 Antenna Radiation Pattern at 2.4GHz	59
Figure 4.70 S11 of the stacked microstrip patch antenna (substrate 5870)	60
Figure 4.71 Antenna Radiation Pattern at 1.8GHz	60
Figure 4.72 Antenna Radiation Pattern at 2.4GHz	61
Figure 4.73 3D Radiation Pattern at 1.8 GHz (5870)	61

Figure 4.74 3D Radiation Pattern at 2.4GHz (5870)	62
Figure 4.75 Antenna Radiation Efficiency (5870).....	62
Figure 4.76 Antenna Total Efficiency (5870).....	63
Figure 4.77 Coax Connection	64
Figure 4.78 Antenna (LP) vs. Antenna (CP).....	64
Figure 4.79 Patch Antenna Axial Ratio	65
Figure 4.80 Fabricated Antenna (Front)	66
Figure 4.81 Fabricated Antenna (back)	66
Figure 4.82 Antenna shorting Test.....	67
Figure 4.83 Antenna placed in the anechoic chamber	67
Figure 4.84 Measured return loss of stacked proximity coupled antenna	68
Figure 4.85 Measured gain in the azimuth plane(1.75ghZ).....	69
Figure 4.86 Measured gain in the azimuth plane (2.4ghZ).....	69
Figure 4.87 Measured gain in the elevation plane(1.75ghZ)	70
Figure 4.88 Measured gain in the elevation plane (2.4ghZ).....	70
Figure 4.89 Simulated Vs. Measured Return Loss	71
Figure 4.90 Simulated Vs. Measured Gain (1.8GHz).....	72
Figure 4.91 Simulated Vs. Measured Gain (2.45GHz).....	72

Abstract

Antennas have a wide range of applications in different fields. Some of the antennas are designed for airborne communications while some antennas have vehicular, signal intelligence and ISR (intelligence, surveillance and reconnaissance) applications. Certain antennas are designed for specific applications, which are suitable for particular purpose, but a number of antennas are multi performing and are versatile. These antennas have a number of feeding techniques. For instance microstrip line feeding, microstrip inset line feeding, coaxial line feeding, aperture coupled feeding and proximity coupled feeding line.

In this research project, proximity coupled feeding technique is applied. A circularly polarized stacked dual band microstrip patch antenna is designed with a cavity backed feeding substrate. In order to get the resonances, the width and length of upper and lower patch is varied. In addition, two stacked patches provide good impedance matching. The feeding line and cavity in the ground plays a pivotal role in getting the required resonances of interest at the desired bands of frequency. The measured results of the fabricated prototype comply with the simulated results. The dual band stacked patch antenna gives 5.19dBi and 5.59dBi gain at 1.75 GHz and 2.38 GHz respectively. The antenna efficiency is 90% and 75% at both these bands with stable radiation patterns.

Chapter # 01

Introduction

This chapter gives a brief background related to types of antennas and the reason behind selecting proximity coupled feeding in the antenna design to make “Dual band circularly polarized proximity coupled stacked patch antenna for RF Energy Harvesting” as the thesis topic. The techniques behind different feeding types and different antenna structures are also presented.

1.1. Antennas

A special transducer called Antenna converts electric current into electromagnetic (EM) waves and does the same process vice versa. They are able to receive and transmit EM (electromagnetic) fields, which involves IR (infrared radiation), radio waves and microwaves. In radio frequency engineering, antennas are defined as an interaction between microwaves moving in metal conductors navigating through the electric currents and space. If we talk about transmission, the antenna in the form of EM waves radiates electric current as a transmitter supplies current to the antenna terminals and emits that energy. Meanwhile in reception, the antenna grabs power from radio waves and produce electric current that is supplied to the receiver at the terminals necessary to amplify. In addition to transmission and reception of radio waves, antennas also perform as an advanced wireless device that optimizes and accentuates radiated energy in some particular direction while subdues it in other directions. Therefore, an antenna behaves like a probing device as well. In wireless communication, antennas are one of the most important components. If an antenna is well designed, it can improve the overall system performance. All radio equipment essentially involve the use of one or more antennas.

Any antenna design can be made once all the requirements are known. Antennas can be made to accept and channel radio waves in a specific direction or in all direction. This particular direction can be high gain, beam or directional antenna. Radio wave antennas and microwave antennas are widely used in our everyday lives. In comparison, visible light antennas and infrared antennas are less common. Although they are used in many places but the type tends to be specialized.

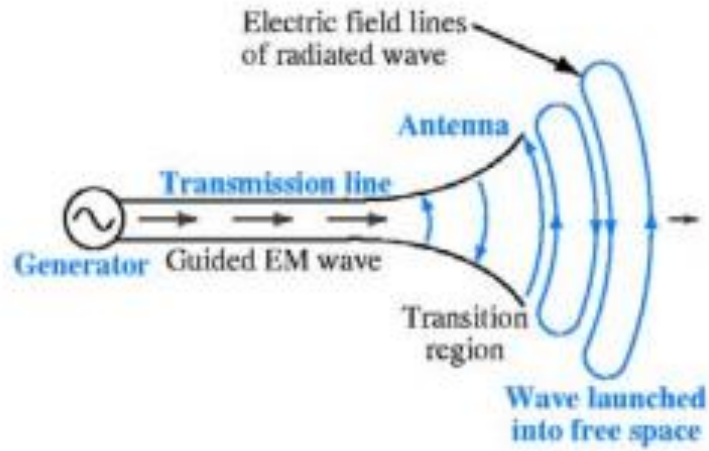


Figure 1.1 Antenna as a transition device

1.2. Types of Antennas

This section discusses some various forms of antenna types and how they are designed to be used in several applications.

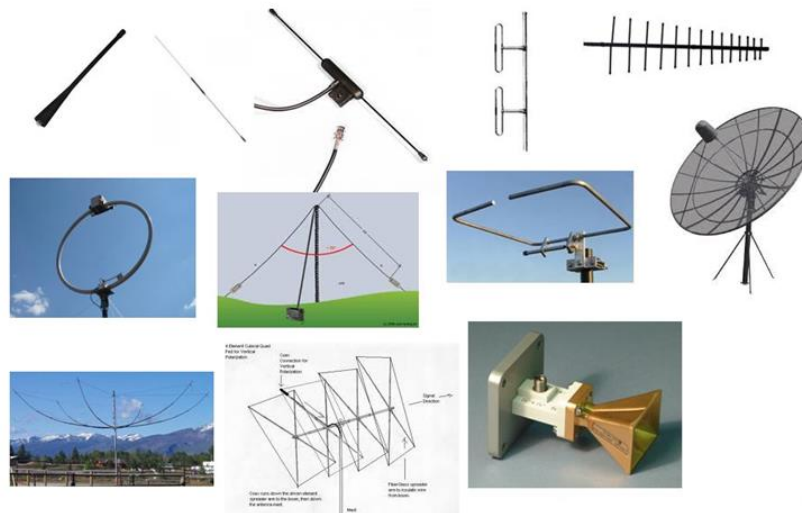


Figure 1.2 Types of Antennas

1.2.1. Wire Antennas

These kind of antennas are widely known because they have several applications in automobiles, spacecraft, buildings, ships etc. These antennas can be made in several shapes such as loop, helix, and dipole (straight-wire). Antennas designed in loop form doesn't necessarily have to be circular in shape. They can be made in either rectangular shape, square shape or ellipse shape. Commonly, circular shape is designed because of ease and simplicity in its construction.

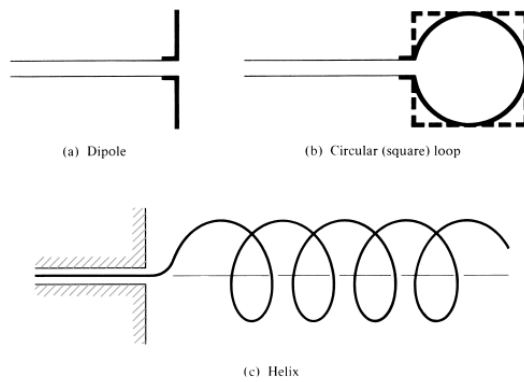


Figure 1.3 Wire Antennas

1.2.2. Aperture Antennas

Today more people have an idea of aperture-coupled antennas than people do in the past. Reason is the increase in the demand of more versatile and sophisticated antennas for modern applications catering to higher frequencies. Typically, these type of antennas are used in spacecraft and aircraft applications. Furthermore, these antennas can be placed under a cover of dielectric material that will secure them from harmful outdoor conditions.

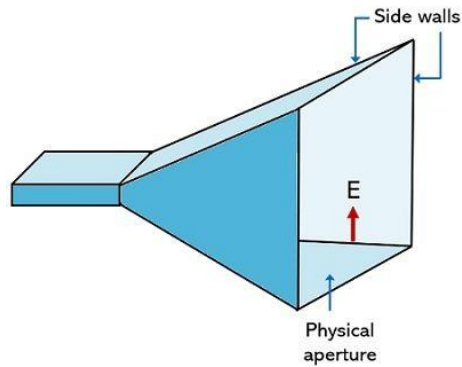


Figure 1.4 Aperture Antennas

1.2.3. Microstrip Antennas

In the year 1970s, Microstrip antennas became immensely popular because of their space borne applications. Now these antennas are used commercially as well as in government sector. The design of these antennas is very simple. A ground substrate encapsulates a metallic patch. This metallic patch can have a number of configurations. Commonly, circular and rectangular patches are used as they are easy to fabricate and can be analyzed in a detailed manner. In these configurations, antenna radiation patterns can be studied efficiently and cross polarization radiation can also be examined effectively. Microstrip patch antennas are cost efficient and easy to fabricate as they have low profile and they comply with planar, non-planar surfaces. These ready to use antennas can be placed on the surface of space probes, ballistic capsules, cars, satellites and mobile phones.

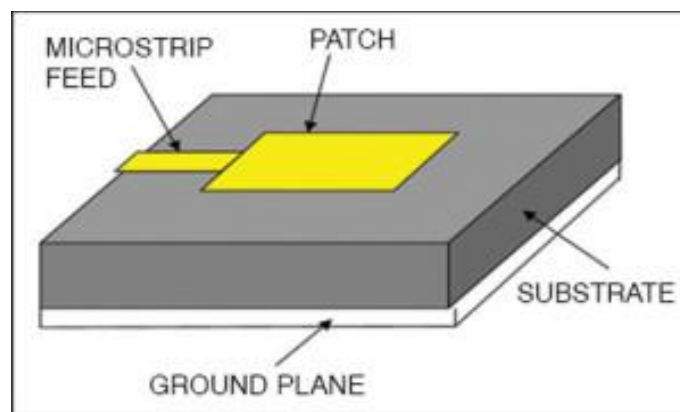


Figure 1.5 Microstrip Antennas

1.2.4. Array Antennas

Some applications insist on radiation characteristics that a single antenna element cannot achieve. Hence, the single element is then transformed into a sum of radiating elements defined in an electrical arrangement and a geometrical pattern. The resulting radiation patterns are the desired characteristics. This particular arrangement will maximize the radiation patterns in the specific direction or minimize it in other directions.



Figure 1.6 Antenna Arrays

1.2.5. Reflector Antennas

These kinds of antennas are used as reflectors. The need to communicate over larger distances in outer space and to be able to receive and transmit signals that had to travel over long miles resulted in reflector antennas. One such common type is parabolic reflectors. These types of antennas are usually built with diameters more than 305m. With such huge dimensions, the high gain of antenna is easily achieved and signals transmit and receive successfully. Another common type of reflector antennas is corner reflectors.

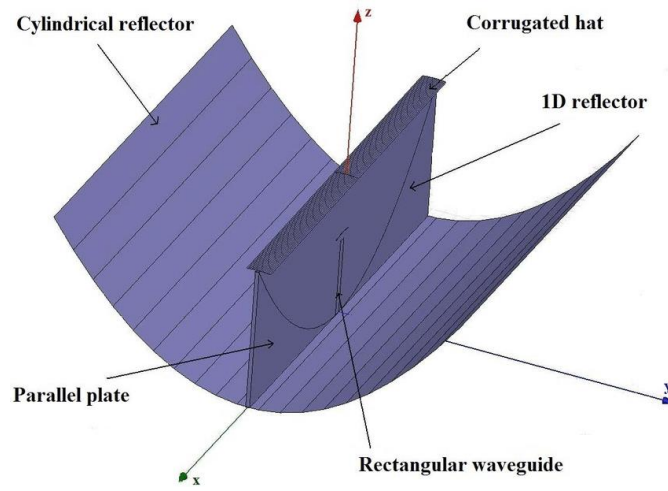


Figure 1.7 Reflector Antenna Arrays

1.2.6. Lens Antennas

This antenna type uses lens to confine the incident energy from splitting it in other unwanted sources. If a proper geometry and lens shape is used, these antennas can convert several forms of differing energy into plane waves. Above-mentioned applications such as ballistic capsules, aircrafts, and missiles can use lens antennas. Lens antennas are commonly used for higher frequencies. Lens antennas are divided into several other categories based on the material from which they are built, or according to their geometry.

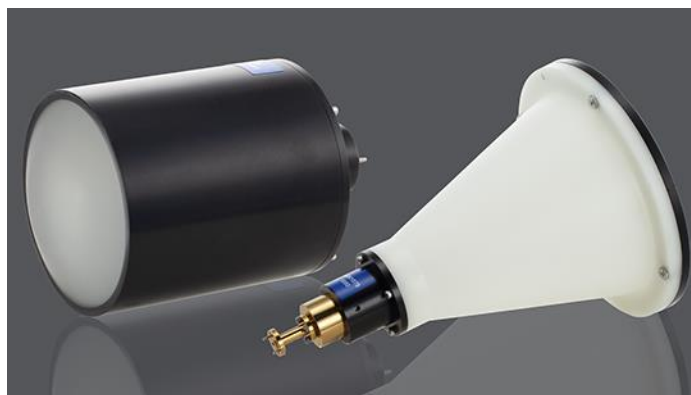


Figure 1.8 Horn Lens Antenna

1.3. Antenna Radiation Pattern

Antenna radiation pattern is its graphical representation or a mathematical function of it's near and far fields. It can be described in terms of space coordinates. Typically, it is determined in the later region. Radiation pattern includes radiation intensity, gain, directivity, axial ratio, polarization phases, power density and field strengths. A trace of the EM field received by the antenna is termed as amplitude field pattern while a graph of constant radius power density is called as amplitude power pattern. Both these fields are normalized which yields normalized radiation patterns.

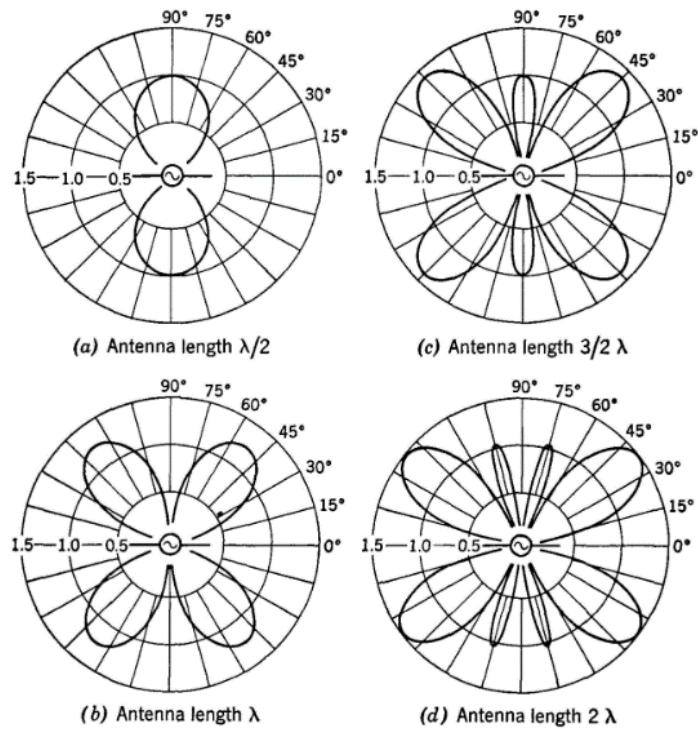


Figure 1.9 Radiation Patterns in free space of periodic straight wire antenna

1.3.1. Field Pattern

It generates magnitude plot of the electromagnetic field described as an angular space function.

1.3.2. Power Pattern (Linear Scale)

It generates square plot of the EM field magnitude as an angular space function in linear scale.

1.3.3. Power Pattern (dB Scale)

It generates square plot of the EM field magnitude as an angular space function in dB scale.

1.4. Radiation Pattern Lobes

Antenna Radiation pattern contains several parts that are divided in to lobes. The sub categories include major, minor, back and side lobe.

1.4.1. Major Lobe

It is defined as the radiating lobe, which contains direction of highest radiation. Some antenna types have more than one major lobe e-g splitting beam antennas.

1.4.2. Minor Lobe

Every other lobe of antenna radiation pattern apart from major lobe is a minor lobe.

1.4.3. Side Lobe

This lobe radiates in any direction apart from minor lobe.

1.4.4. Back Lobe

This lobe radiates where the axis is at 180' to that of antenna beam. Normally a back lobe refers to as a minor lobe when it involves the semi-circle of the major lobe in the opposite direction.

1.5. Radiation Power Density

It is defined as a relationship between power and associated electromagnetic waves given as instantaneous Poynting vector by the equation:

$$W = E \times H \quad (1.1)$$

When,

$$W = \text{instantaneous pointing vector (w/m}^2\text{)}$$

$$E = \text{Instantaneous electric-field intensity (V/m)}$$

$$H = \text{Instantaneous magnetic field intensity (A/m)}$$

1.6. Radiation Intensity

It is defined as “radiated power of an antenna in a given direction per unit of solid angle”. It is a parameter of far field and it can be obtained through multiplying distance square with radiation intensity of the antenna like the equation below:

$$U = r^2 W_{rad}$$

1.7. Beam width

Beam width is linked with the antenna radiation pattern and is given by separation between two identical angular points on the maximum pattern of the opposite side.

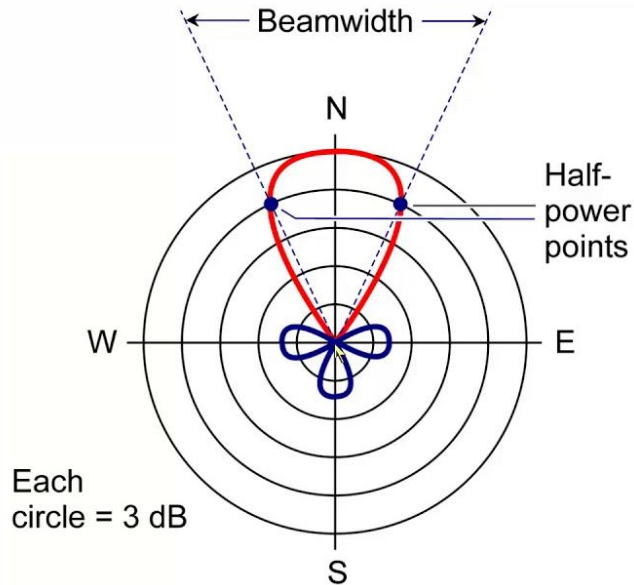


Figure 1.10 Beam width of an antenna

1.8. Directivity

Antenna directivity is the ratio of radiation intensity in a particular direction to that of radiation intensity over all other directions of antenna. Average radiation intensity is equal to the total radiated power divided by 4π by the antenna. If a specific maximum direction of radiation is not given then the direction of maximum intensity of radiation is applied. Mathematically:

$$D = \frac{U}{U_o} = \frac{4\pi U}{P_{rad}} \quad (1.2)$$

If a specific maximum direction of radiation is not given then the direction of maximum intensity of radiation is applied given as:

$$D_{\max} = D_o = \frac{U_{\max}}{U_o} = \frac{4\pi U_{\max}}{P_{rad}} \quad (1.3)$$

Here D =Directivity

D_o =Maximum Directivity (dimensionless)

U =radiation intensity

U_{max} =Maximum Radiation Intensity

U_o = Isotropic sources radiation intensity

P_{rad} =Total radiated power (W)

1.9. Beam Efficiency

Beam efficiency is another factor used to describe antenna's power of transmitting and receiving signals. It is given as:

$$BE = \frac{\text{Power transmitted within cone angle } \theta}{\text{Power transmitted by the antenna}} \quad (1.4)$$

1.10. Bandwidth

Antenna bandwidth is the set of frequency range under which the performance of an antenna is measured abided by special standards. It can also be taken as set of frequency range on one side of fundamental frequency around where the antenna characteristics is acceptable. For narrowband antennas, the bandwidth given by a percentage of the frequency difference. Proper adjustments of dimensions can increase the acceptable frequency range of these antennas. Radios installed in cars and television sets are common examples of tuning an antenna for better reception of signals. This can be done by adjusting lengths of antenna to an acceptable frequency range.

1.11. Gain

Gain and Directivity of the antenna are interlinked with each other. It involves both the efficiency and direction of the antenna. Gain is the ratio of radiation intensity in one direction to that of radiation intensity of an isotopically radiated antenna. Mathematically:

$$\text{Gain} = 4\pi \frac{\text{radiation intensity}}{\text{total input power}} = \frac{4\pi U(\theta, \phi)}{P_{in}} \quad (\text{dimensionless}) \quad (1.5)$$

1.12. Antenna Efficiency

It is the total efficiency due to losses at the entry terminals around the structure of an antenna. This can occur may be due to reflection (Antenna and transmission line mismatch), conduction losses and dielectric losses etc. Mathematically:

$$\epsilon_o = \epsilon_r \epsilon_c \epsilon_d \quad (1.6)$$

Here,

$$\epsilon_o = \textit{Total Efficiency}$$

$$\epsilon_r = \textit{Reflection mismatch}$$

$$\epsilon_d = \textit{Dielectric Efficiency}$$

1.13. Input Impedance

It is the ratio of voltage to current at the entry terminals of an antenna or the impedance presented by the antenna at its loading terminals. It can be described as appropriate ratio between electric and magnetic fields at the point. Mathematically:

$$Z_A = R_A + jX_A \quad (1.7)$$

Here,

$$Z_A = \textit{antenna impedance at terminals}$$

$$R_A = \textit{antenna resistance at terminals}$$

$$X_A = \textit{antenna reactance at terminals}$$

1.14. Polarization

It is the polarization of the radiated or transmitted wave in a given direction by the antenna. If the direction is not specified then it may be in the direction of highest gain. It is further divided into linear, circular and elliptical polarization.

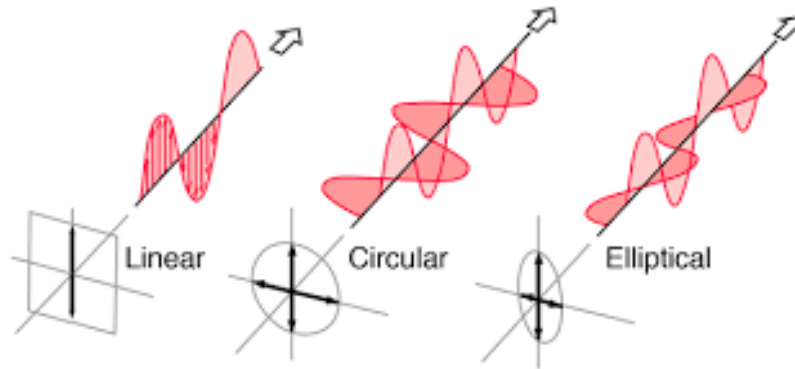


Figure 1.11 Classification of Polarization

1.14.1. Linear Polarization

Linear polarization of an antenna is referred as EM field vector that traces a line as long as the time progresses. It is further classified into vertical polarization, horizontal polarization and slant polarization.

1.14.1.1. Vertical Polarization

Type of linear polarization in which the EM fields are perpendicular to the earth's surface is called Vertical Polarization. Its angle of radiation is very close to earth's surface. Antennas that are vertically polarized with single vertical elements are able to radiate the electric and magnetic field equally in the horizontal planes. Some common examples of vertically polarized antennas are AM radio broadcasting towers and whip antennas in automobiles.

1.14.1.2. Horizontal Polarization

Type of linear polarization in which the antenna radiates electromagnetic lines in horizontal plane is called Horizontal Polarization. Antennas that are horizontally polarized radiate the electromagnetic lines parallel to the surface of the earth. A common example of horizontal polarization would be antennas used in television sets.

1.14.2. Slant Polarization

Type of linear polarization in which the antennas radiates either vertically or horizontally is called slant polarization. In this category, the antenna can be either vertically polarized or horizontally polarized to receive or transmit signals. The radiation angles are $+45^\circ$ and -45° in slant-polarized antennas.

1.14.3. Circular Polarization

Circular polarization of an antenna is referred to as EM fields that track down a circle as a time function. The following conditions are necessary in order to meet the circular polarization:

1. The EM fields must have two linear orthogonal components.
2. Both components should have same magnitude.
3. Both components must have a time phase difference of 90 odd multiples.

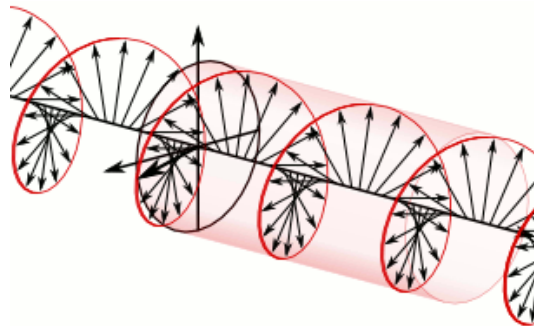


Figure 1.12 Circular Polarization

1.14.4. Elliptical Polarization

Elliptical polarization of an antenna is referred to as EM fields that track down an elliptical module in space. Its right hand EP if the field vector rotates in a clockwise manner and left hand EP if the field rotates an anti-clockwise manner. In addition to using rotation of field to determined polarization a rule is set for circular polarization, elliptical polarization. It can be determined using the antenna axial ratio which is ratio of major to the minor axis. The following are the conditions necessary to meet the criteria:

1. The EM field should have two linear orthogonal components.
2. Both components can have same or different magnitude.
3. If both components do not have same magnitude, then phase difference of time must be multiples of π or should not be π .

1.15. Friis Equation of Transmission

The design of practical communication systems demands the use of this equation. It is the power received to power transmitted between two antennas that are separated by distance. It also helps

in the design of space communication systems. It is helpful in selecting antennas with correct gain. It is used in antenna measurement setup. It also helps in estimating the coverage area, selecting the power levels of transmitter and receivers.

$$\frac{P_r}{P_t} = (1 - |\Gamma_t|^2)(1 - |\Gamma_r|^2) \left(\frac{\lambda}{4\pi R}\right)^2 G_t G_r |P_t \cdot P_r|^2 \quad (1.8)$$

1.16. Feeding Methods

There are several feeding techniques available by the help of which antenna is excited. The selection of choosing a feeding technique is important because it will then decide the return loss of antenna along with antenna radiation characteristics such gain, directivity, polarization, bandwidth and antenna efficiency. Moreover, if the substrate thickness is increased it will directly hamper antenna bandwidth and result in increase of the surface waves. These techniques are classified into two categories.

- 1) Contacting Feeding Method.
- 2) Non-Contacting Feeding Method.

1.16.1. Contacting Feeding Method

This feeding method involves RF power, which is directly applied, to the radiating patch by the help of a connecting element. Either this element can be a microstrip, a coaxial probe or an inset fed/notch fed which are also popularly used.

1.16.1.1. Microstrip Feeding Method

This technique of feeding involves a conducting strip, which is connected to the boundary of the microstrip patch directly. Thus the patch and the feed can be designed on the same substrate making it a planar structure.

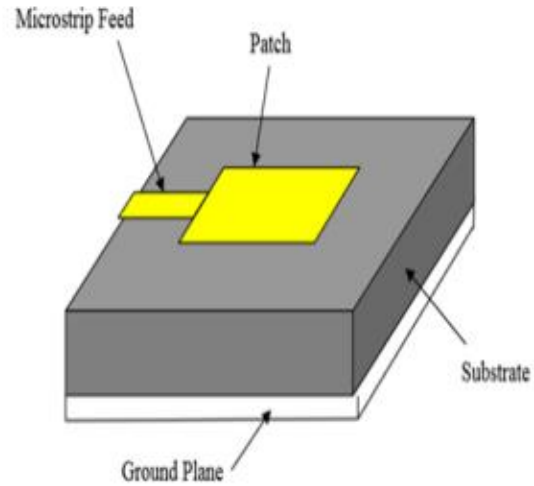


Figure 1.13 Microstrip Fed Patch Antenna [1]

1.16.1.2. Coaxial Feeding Method

This technique of feeding is also called probe feeding. Here an inner conductor of the coaxial probe is connected to the dielectric substrate and is soldered on the radiating patch meanwhile the outer conductor is grounded.

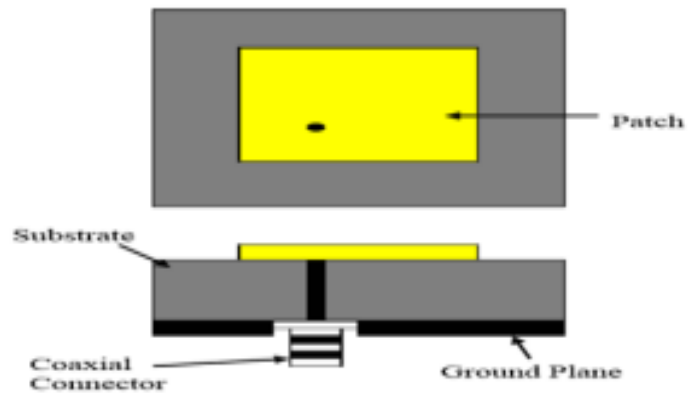


Figure 1.14 Coaxial fed patch antenna [1]

1.16.2. Non Contacting Feeding Method

This feeding method involves RF power, which is indirectly applied through electromagnetic field coupling by using either aperture coupling or proximity coupling to transfer power between the microstrip.

1.16.2.1. Aperture Coupled Feeding Method

This feeding method involves the use of two different substrates that are put in together to give EM coupling from the feed to the patch that is radiating. The thickness of these two substrates and their subsequent dielectric constant must be kept separate to ensure proper electrical functions and circuitry. The radiating patch is mounted on the top of antenna meanwhile the microstrip feed line is placed on the feeding substrate bottom which gives aperture coupling. The feed line is designed in the patch center to ensure less cross polarization.

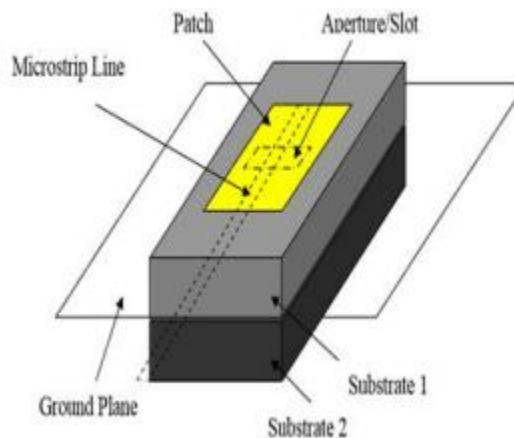


Figure 1.15 Aperture coupled fed patch [1]

1.16.2.2. Proximity Coupled Feeding Method

In this feeding method, as mentioned above in aperture coupling two substrates are sandwiched to produce multiple resonances. The feeding line is designed between the substrate and the ground. On top of upper substrate, a radiator patch is mounted. This helps in the reduction of spurious feed radiation resulting in higher bandwidth. The two substrates used in this technique may have same dielectric or different depending upon the application of the antenna where it is

used. The disadvantage of using this technique is that the fabrication is hard and requires both the dielectrics to be properly aligned.

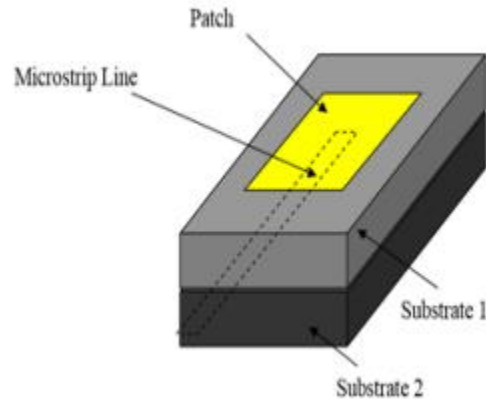


Figure 1.16 Proximity fed patch antenna [1]

1.17. RF Energy Harvesting

Electromagnetic energy is captured from a radio frequency spectrum and is converted into usable electrical domain in a process, which is known as RF energy harvesting. To be specific, RF energy harvesting is relevant in wireless communication systems where there are loads of RF signals present in abundance in the environment. It requires low power sensors for the devices to be wirelessly powered and used in various applications. However, it is an arduous task for the designers to extract energy from RF sources, as they are present at the junction between EM fields and electronic circuitry. It involves the use of antennas one of which is discussed in the following chapters. These antennas then convert the extracted RF signals into electrical energy by means of rectification. The output from the rectifier is utilized to empower various electronic devices or charging a battery for use later. RF energy harvesting involves a number of frequency bands to harvest energy from depending upon the application and availability but essentially it targets GSM, Wi-Fi and Bluetooth frequency bands as they are commonly used. In this thesis, the researcher aims to target GSM 1800 MHz and Wi-Fi 2.4 GHz frequency bands. Commonly, RF energy harvesting is used in IoT devices and other low power sensors and actuators [16]. It is used in empowering wearable electronic devices. It can also be used in remote monitoring systems. Here the challenge lies in attaining power level as the signals present in the environment are low and it can result in poor efficiency. As the RF signals are harvested from

the environment so strength and vicinity of the RF source is important and inclusion of other RF devices can cause hindrance in the overall system efficiency.

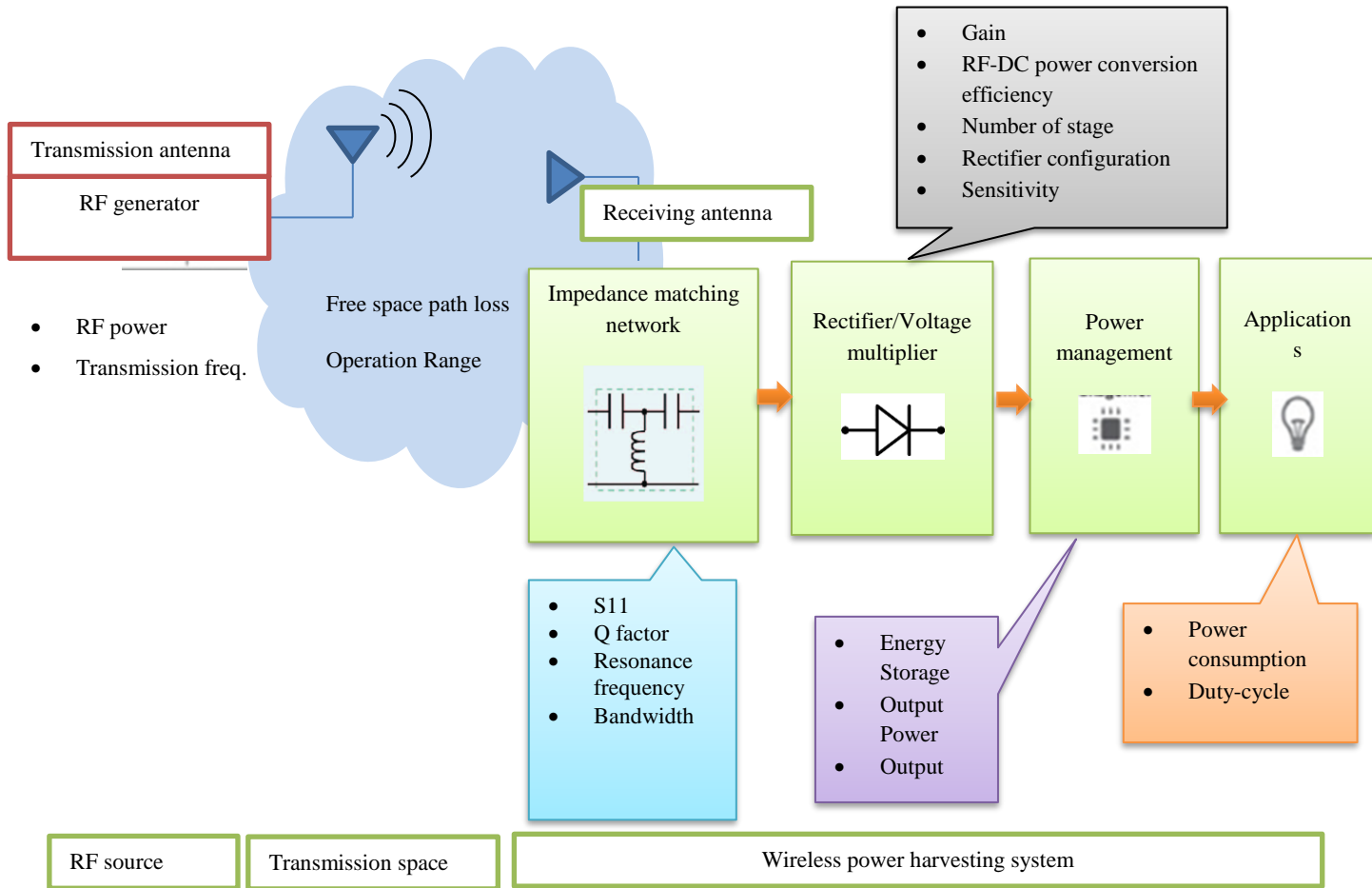


Figure 1.17 RF Energy Harvesting

1.17.1. Incorporation with other technologies

This technology can be combined with other technologies such as solar energy or piezoelectric energy to improve the energy capture and increase in efficiency of the system overall. Today better antennas, rectifiers and energy storage devices are employed for best results in the field of RF energy harvesting. This corresponds to incorporating licensed RF bands to harvest energy from in order to avoid involvement with the communication systems.

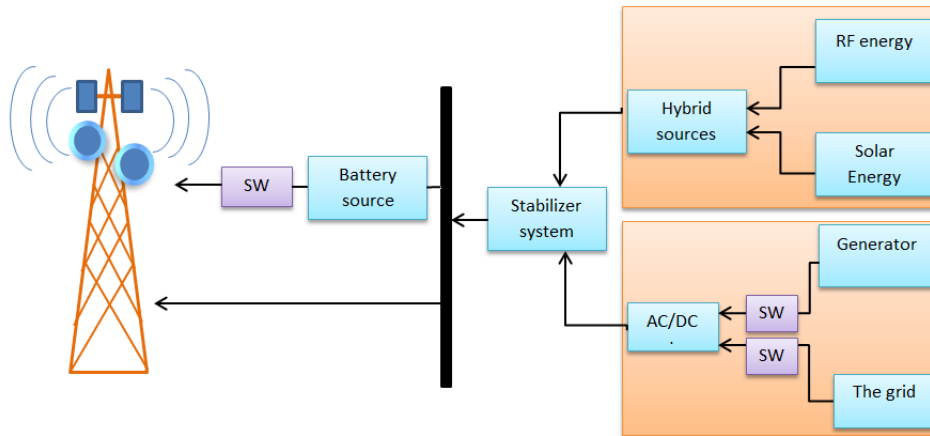


Figure 1.18 Hybrid Energy harvesting system model with solar and RF energy

1.18. Thesis Objectives

The objectives of the subject research are listed below:

- A multilayer microstrip patch antenna for ambient RF energy harvesting.
- To incorporate proximity coupled feeding for wider bandwidth.
- To achieve multi bands at GSM 900 and Wi-Fi 2.4 GHz.
- To achieve circular polarization on the antenna.
- To achieve antenna efficiency greater than 90%.
- To fabricate and test the antenna design.

1.19. Advantages

The advantages of given thesis will be:

- Multilayer structure will be compact size and good at providing RF energy harvesting.
- Proximity coupling technique has low surface wave losses.
- Proximity feeding also produces linear and circular polarization in contrast to coaxial feeding.

1.20. Areas of Application

This thesis project is relevant to national needs and can be utilized in following domains:

- Iot devices
- RF Energy harvesting companies (Mica Energies, Otego etc.).

Chapter # 02

Literature Review

In this chapter, different papers are discussed in detail related to matching networks and RF energy harvesting. These papers have also been implemented and thoroughly studied over the course of research. The chapter also includes a detailed literature review table to present the direction of research in tabular form.

2.1. Background

Impedance matching involves simple but complex engineering, as it is able to transform power from a source to load and then reduce reflections coming from a signal to load. Today, we are dealing with wireless technology and everywhere there is less cables, hardware, and more minimal PCBs, which involves the use of inverters, amplifiers, oscillators, rectifiers, power dividers etc. Today, system demands high impedance matching networks. For that purpose, we deploy a number of techniques for designing an impedance matching network. In this regard, power amplifiers and rectifiers normally use nonlinear elements in the circuits i-e transistors and diodes so that their input impedance change according to the frequency, load impedance and power at the input. Contrary to this, it is challenging to design nonlinear circuits for impedance matching network. Nowadays wireless harvesting of energy and wireless transfer of power has been getting many eyes. Whether inductive or radiative wireless power transfer, rectifiers play a pivotal role in converting RF to DC or AC to DC, which makes impedance matching networks gain high antenna conversion efficiency. An antenna that is working as a rectifier is an important device used for both wireless power transfer and wireless harvesting of energy applications. So far, significant progress has been seen in designing broadband Rectenna and multiband Rectenna, which are able to harvest RF energy and receive power from different channels making them superior to perform over single band rectifying antennas taking their total input power and overall conversion efficiency into account. In this matter, designing an impedance matching network is an arduous task to perform and thus the structure of these networks is complex resulting in increased cost and more losses. These errors introduce glitches in the manufacturability of the networks. In order to reduce these errors, frequency selective surfaces (FSS) and resistance compression networks are employed in the design. These circuits minimize

the nonlinear characteristics of Rectenna and make them able to work under different operating conditions. Here again, the size and cost of overall design increase which makes the final design complex. So, a simple design with good performance is required involving no complex structures. That's why, matching network should either be eliminated or it is transformed into a simple structure. These simple structures should be able to receive RF power at multiple frequency bands and hold high gain and high efficiency of RF-DC conversion. Some of the designs include a simple 50Ω antenna matched with a rectifier. In these antenna designs, narrow operating bandwidth is observed or broadband low conversion efficiency is observed usually lower than 20%. So we will discuss a novel approach to design a broadband rectifying antenna that will not involve the use of matching network.

2.2. Broadband Rectenna with Matching Network Elimination

This broadband antenna design is center-fed symmetrical dipole, which will then be used to further transform it to OCFD antenna [14]. It can be seen that the bowtie arms of the dipole antenna are shaped in a radial direction to obtain wider frequency bandwidth. This antenna design is another version of a biconnical design of antenna. The characteristic impedance Z_0 is given by:

$$Z_k = 120 l_n \cot\left(\frac{\theta}{4}\right) \quad (2.1)$$

Here θ is the cone angle. Now input impedance of a biconnical antenna is given as:

$$Z_i = Z_k \frac{Z_k + jZ_m \tan\beta l}{Z_m + jZ_k \tan\beta l} \quad (2.2)$$

In this equation, $\beta = 2\pi/\lambda$ (λ is the wavelength of the antenna,

$$l = \text{length of the cone and } Z_m = R_m + jX_m \quad (2.3)$$

The VSWR in the case of these antennas should be less than 2 over a bandwidth of 2:1. The input impedance of bowtie broadband antenna is equal to that of biconnical antennas and the value of input impedance is a function of cone angle, arm length and frequency.

Sr. No.	Theta (θ)	R=40mm	R=50mm	R=60mm
1.	$\theta = 10$	1.93-2.4Ghz	1.83-1.9 Ghz	1.58-1.9 Ghz
2.	$\theta = 20$	1.93-2.8 Ghz	1.75-2.7 Ghz	1.58-1.98 Ghz
3.	$\theta = 30$	1.91-2.5 Ghz	1.73-2.9 Ghz	1.55-2 Ghz
4.	$\theta = 70$	1.91-2.8 Ghz	1.73-2.1 Ghz	1.55-2.3 Ghz

Table 1 Simulated frequency of the broadband antenna

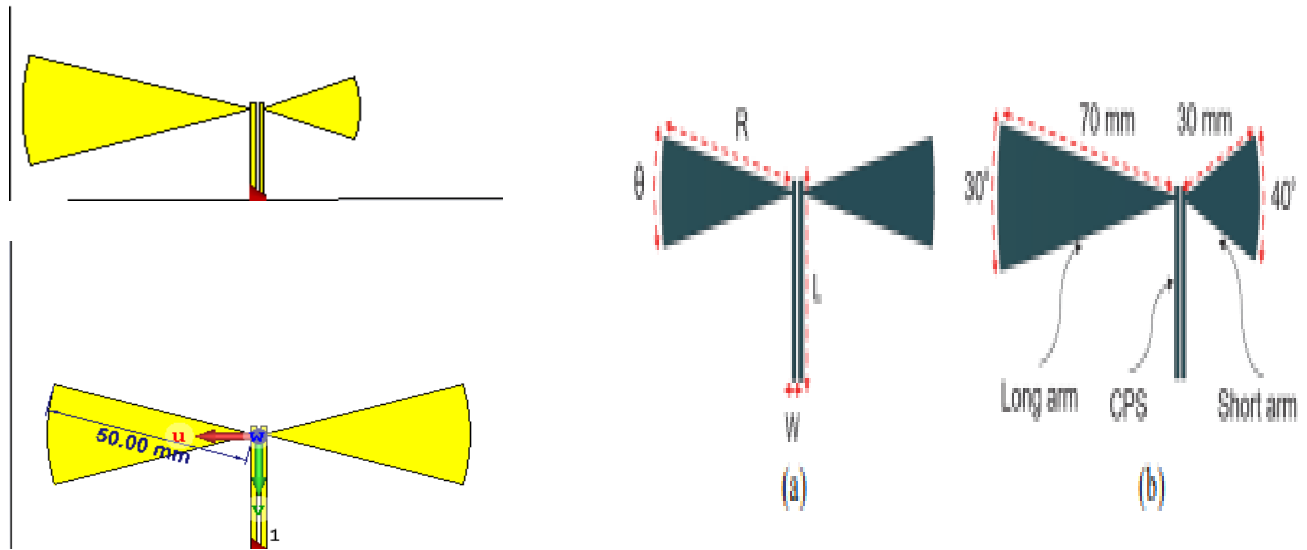


Figure 2.19 CST Design of the broadband antenna [14]

The simulation results of the aforementioned broadband antennas are given below:

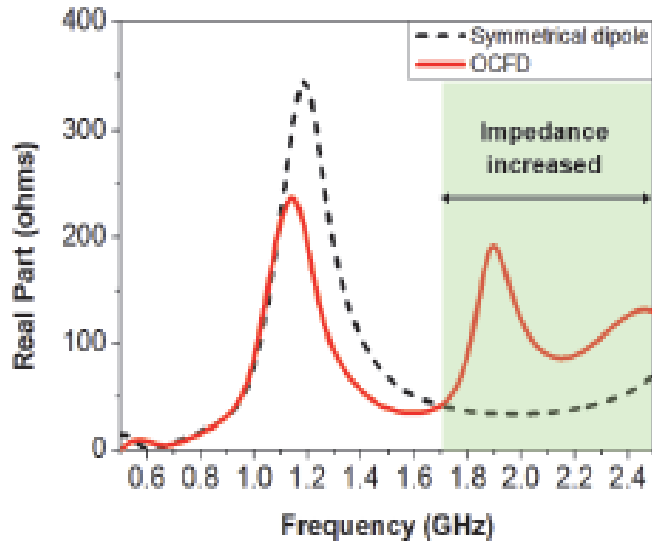


Figure 2.20 Broadband antenna results [14]

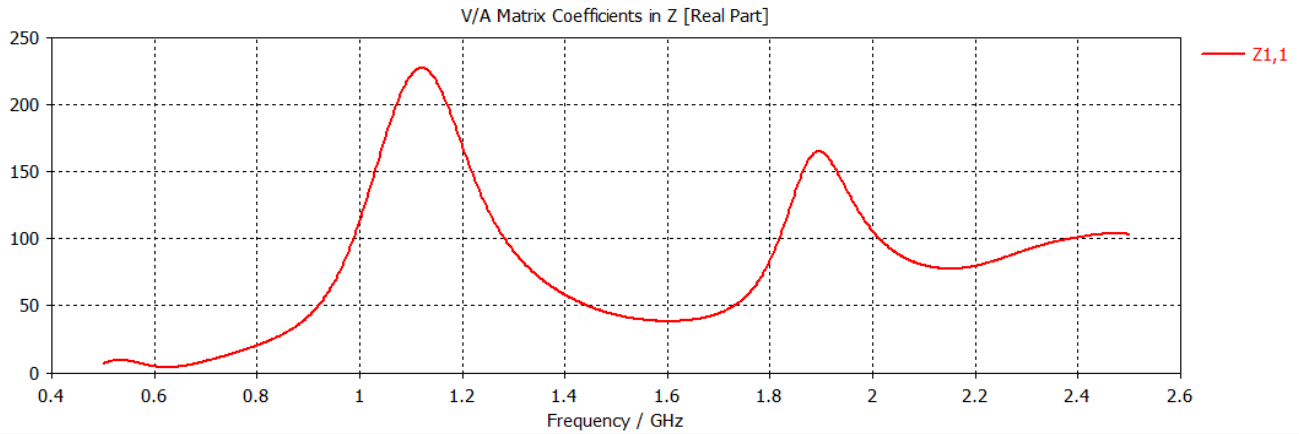


Figure 2.21 Simulated results of the broadband antenna

Now converting this center-fed dipole antenna design into an off-center fed dipole design, the longer arm length is increase to 70mm and the length of arm that is shorter has been reduced to 30mm. To make the antenna symmetric, the circumference angle of the same arm is increase to 40°. The resulting length of the dipole antenna will be around 100mm after this.

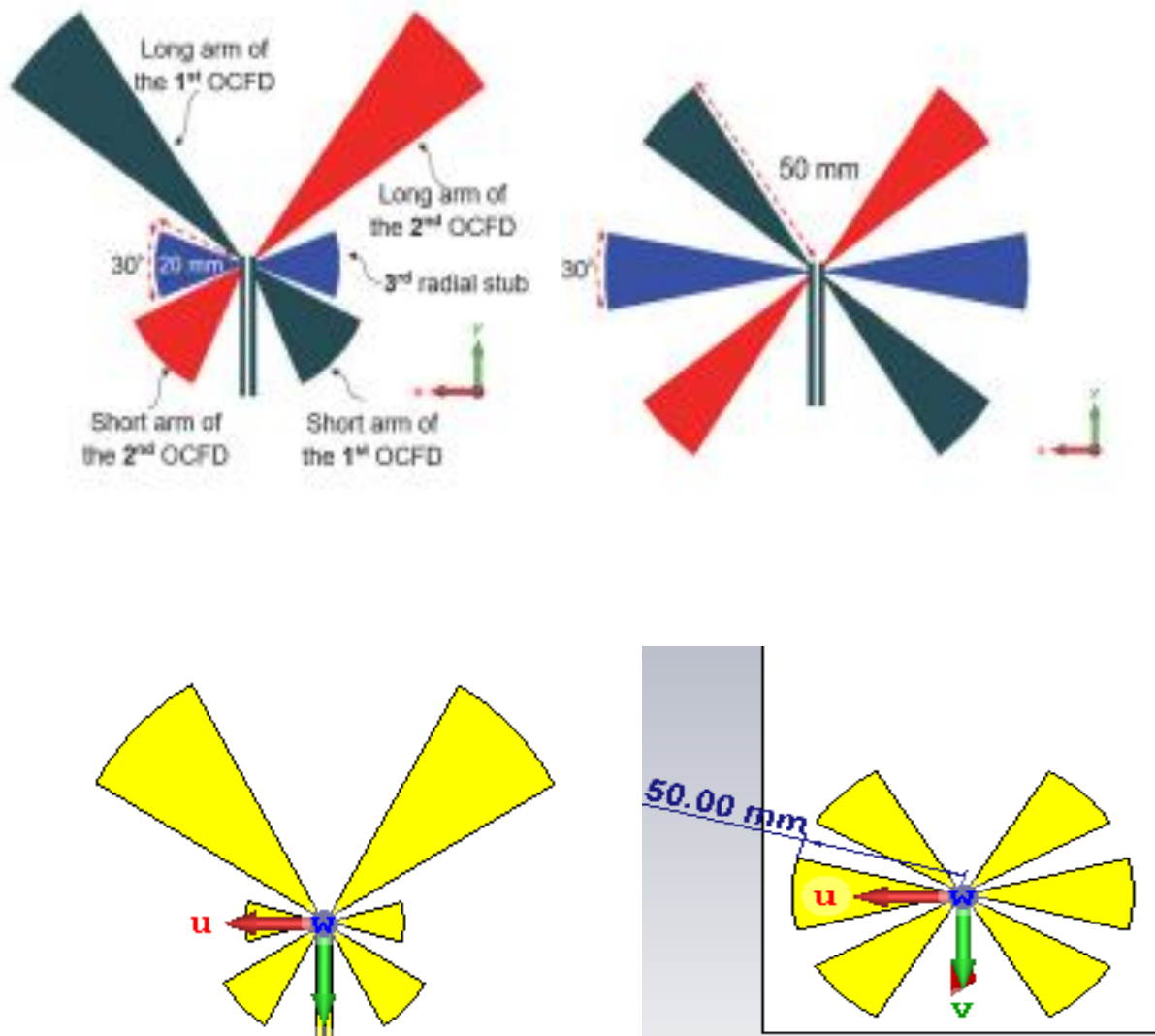
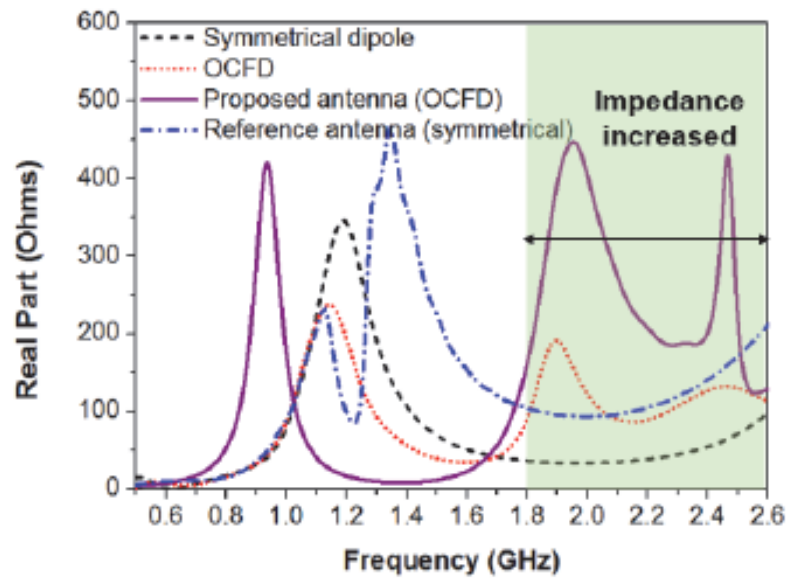


Figure 2.22 Antenna design for OCFD antenna [14]

The simulation results of the above-mentioned four antennas in OCFD configuration is shown below:



(a)

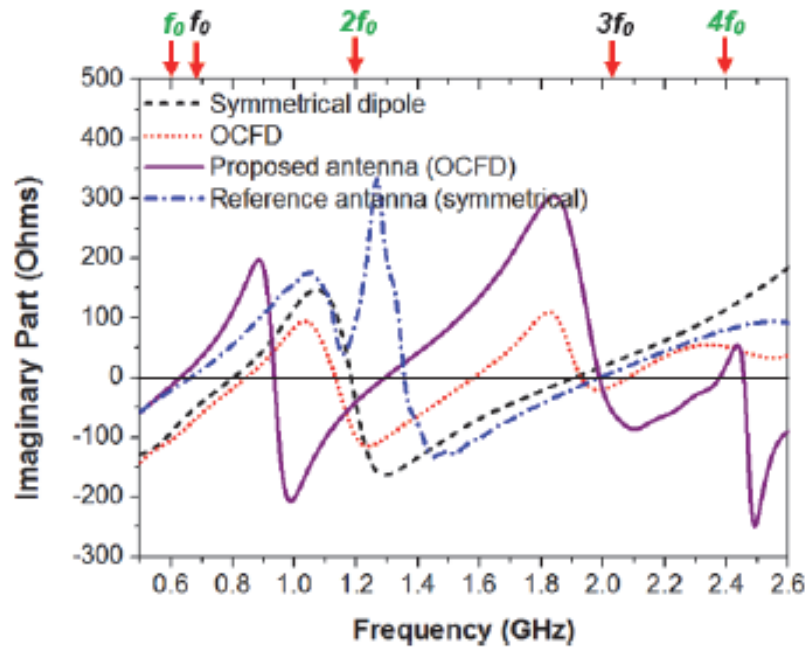


Figure 2.23 Offcentre-fed dipole antenna results [14]

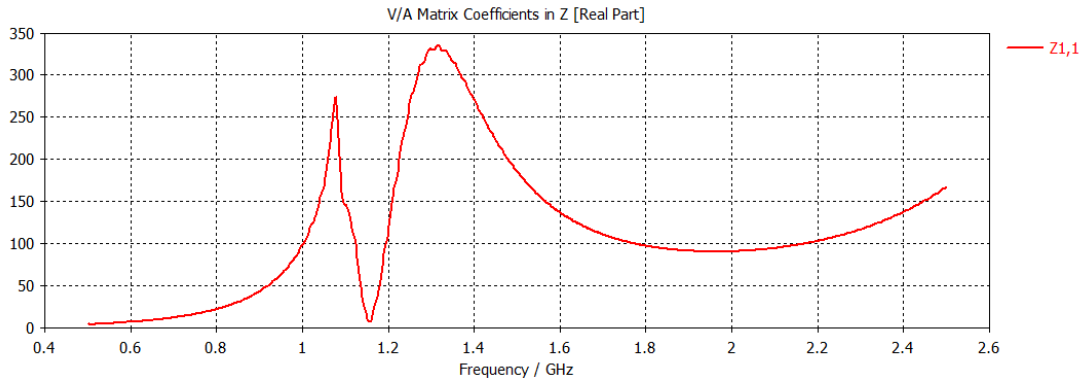


Figure 2.24 Simulated results for off-centre fed dipole antenna

It is interesting to note that the real impedance part of the dipole antenna has increased over the frequency band while that of imaginary part has been kept the same over the resonant frequency band. Also taking into account the dipole antenna impedance is nearly 50Ω around 2nd and 3rd frequency bands between 1.75 and 2.45 GHz which proves the performance of the dipole antenna to have been broadband. Here one major drawback of using a OCFD antenna is that antenna radiation resistance can be too high and it will demand a 4:1 or 5:1 transformer to transform the antenna impedance to match 50 ohms feeding port resistance.

2.3. Novel Broadband and Frequency Selective Rectennas for a Wide Input Power and Load Impedance

The design of this antenna removes the use of complex impedance matching networks. This work involves orchestrating the input impedance of a standard micro strip patch antenna, where the antenna impedance is optimized to match the rectifier impedance at required frequency and reject the unwanted frequencies (harmonic distortion). With this design, broadband frequency selectable antennas can be achieved without the involvement of complex matching network designs [15]. These antennas can be helpful for obtaining energy harvesting and power transfer applications. In this design, a simple patch microstrip antenna is designed having a ground plane. It is cost effective and is fabrication friendly. To adjust the frequency, the antenna is tilted to 60° making it a novel design. After that, four shorting pins are inserted in order to achieve frequency bands at the desired places from the ground plane to the patch. The antenna size is 90×90 with a 64×56 patch on top it. It is made using Rogers 5880 and thickness of the substrate

is 1.58mm. The simulated result of the above mentioned antenna is shown below along with the implemented results on CST software.

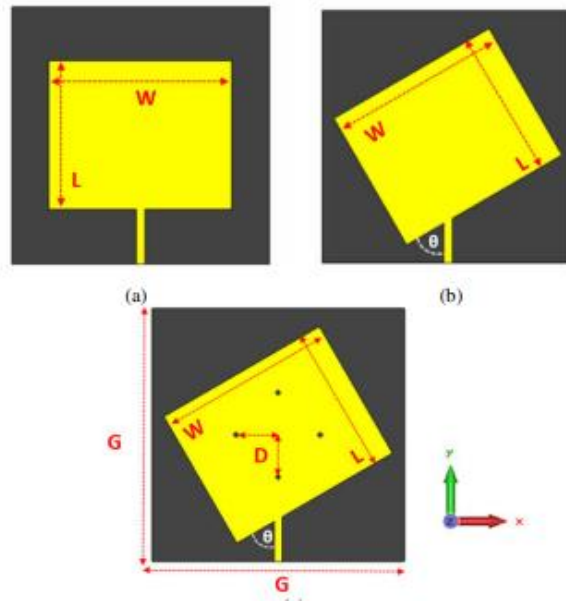


Figure 2.25 Novel Broadband Frequency Selective Rectenna [15]

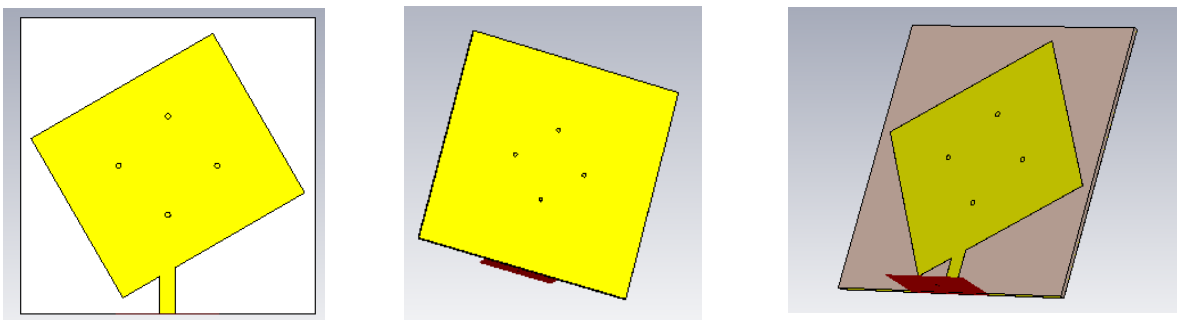


Figure 2.26 CST Design of the novel broadband antenna

The real and imaginary part of the broadband OCFP antenna is shown below:

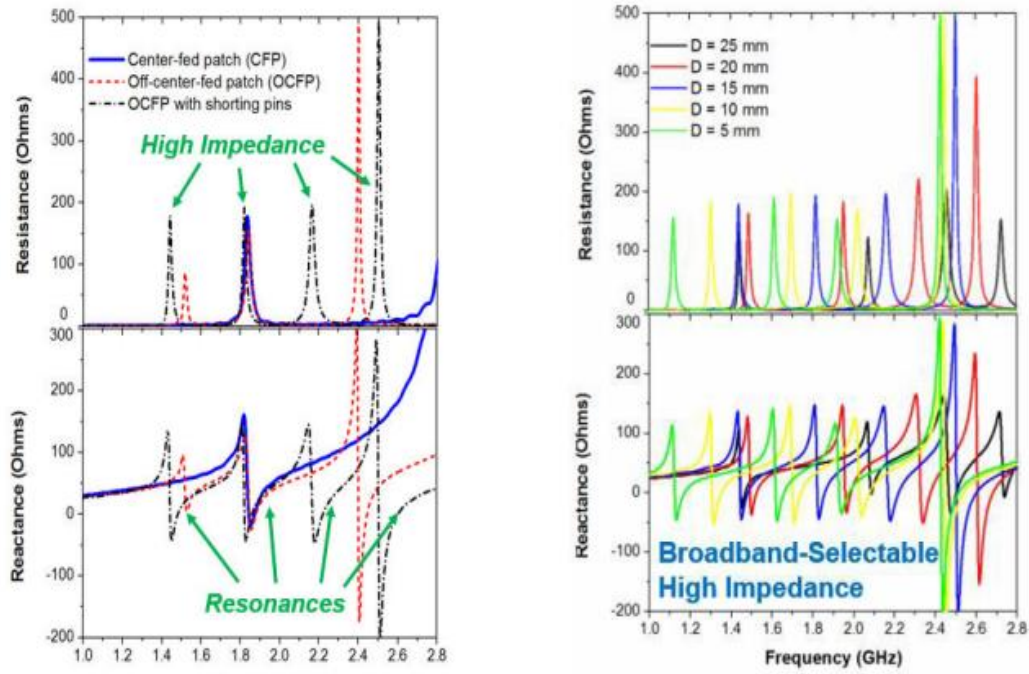


Figure 2.27 Novel Broadband FSS Rectenna results [15]

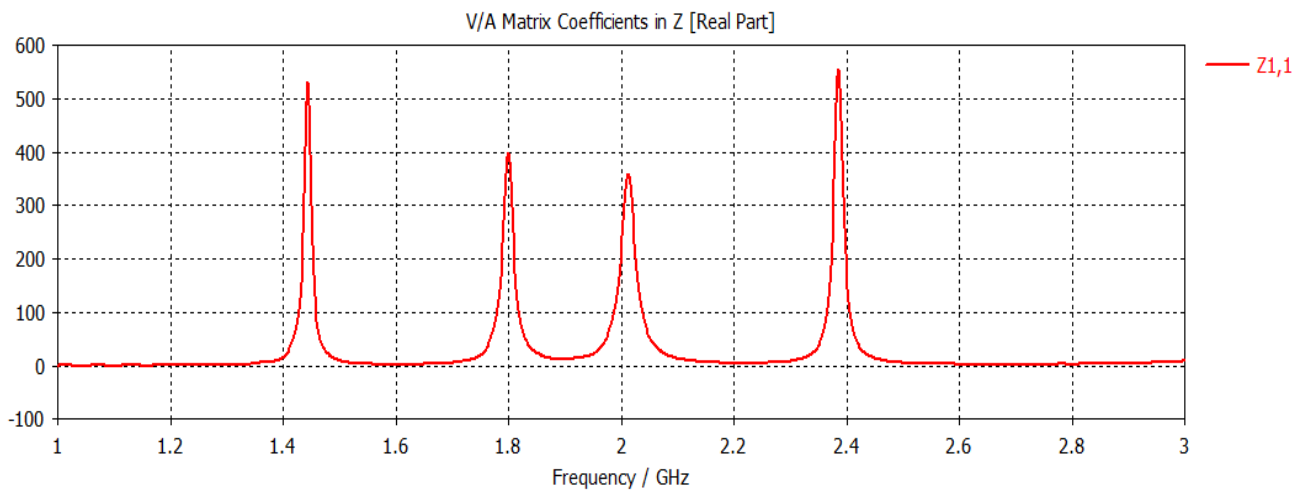


Figure 2.28 Simulated results of Novel Broadband Antenna

After that, the rectifier is made to complete the rectenna design using ADS software. For this purpose, HSMS 2852 schottky diode is employed along with 100nf capacitors and a load resistance of 2000Ω.

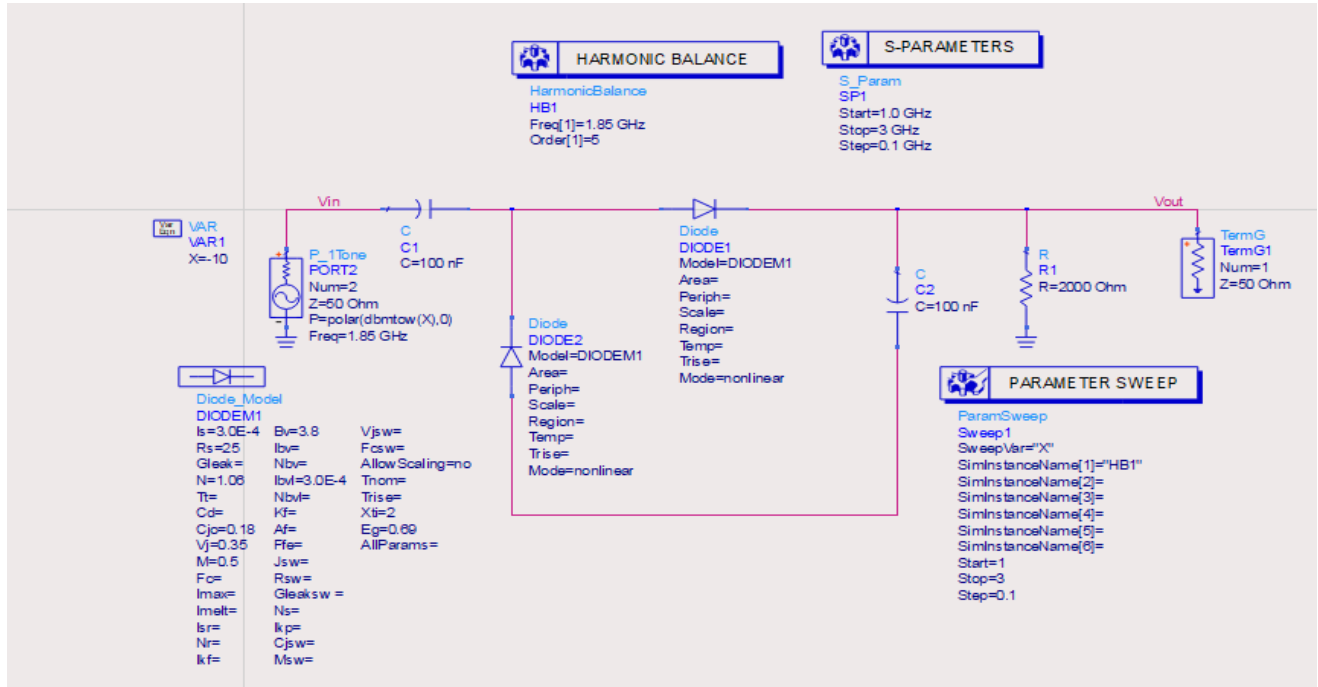


Figure 2.29 ADS design of the rectifier

In this design, two major drawbacks occur:

- 3) The elimination of a matching network results in using more circuit components. So, it will be quite a task to obtain a Rectenna that has high efficiency and which can cover multiple bands of frequency.
- 4) Harmonic signals generated at higher order and cannot be essentially eliminated by the rectifier when the antenna bandwidth is greater than 2:1. ($f_n > 2f_0$). This can decrease overall efficiency of the Rectenna.

2.4. 3D Quad band Array Rectenna for Efficient Energy Harvesting

This work focused on a hybrid approach in combining RF and DC power for empowering Internet of Things (IoT) devices in feasible environments with the help of a 98 MHz FM band antenna and a cross-dipole dual polarized bowtie antenna with asymmetric slots to obtain GSM 900, GSM 1800 and Wi-Fi 2.4 GHz [16]. These antennas are then combined with a power combiner to obtain a 3D cubicle structure and a rectifying circuit to complete the Rectenna

design aimed at providing ambient RF energy harvesting. The 100x100 antenna is made using CST software and is designed using a FR4 substrate. It yields a peak voltage of 2.38V at -10dBm and gives good results both in indoor and external environment setups. The antenna along with the rectifier is shown below with its implemented design and results.

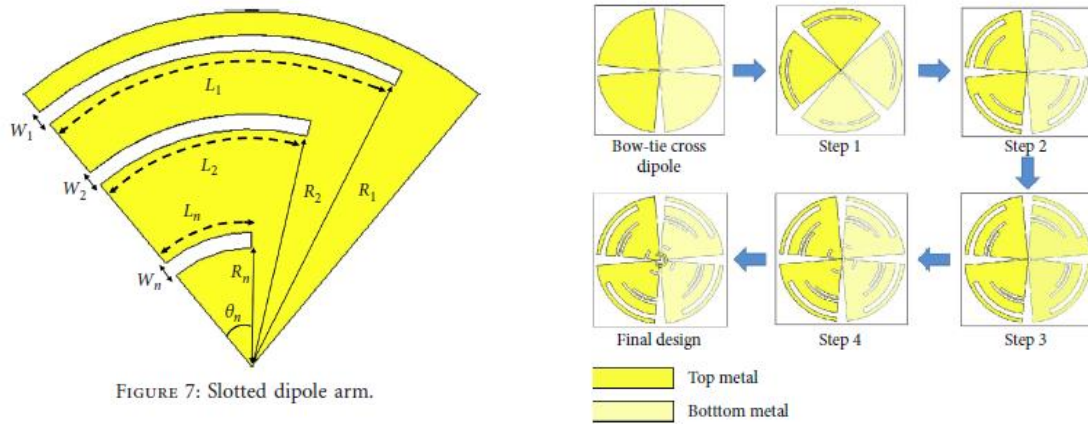


Figure 2.30 Bowtie Antenna for energy harvesting [16]

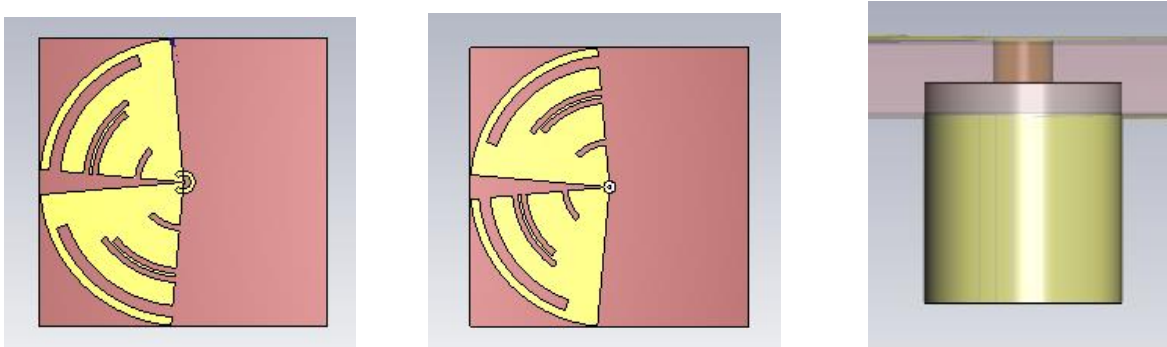


Figure 2.31 CST Design of the Bowtie Antenna

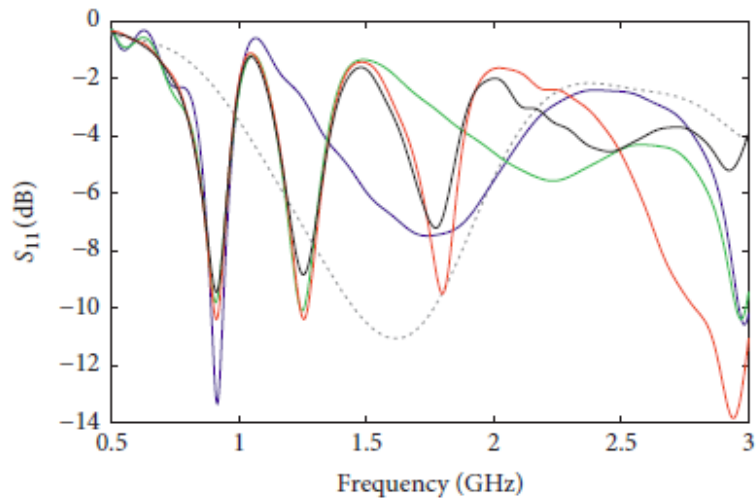


Figure 2.32 Bowtie Antenna Results [16]

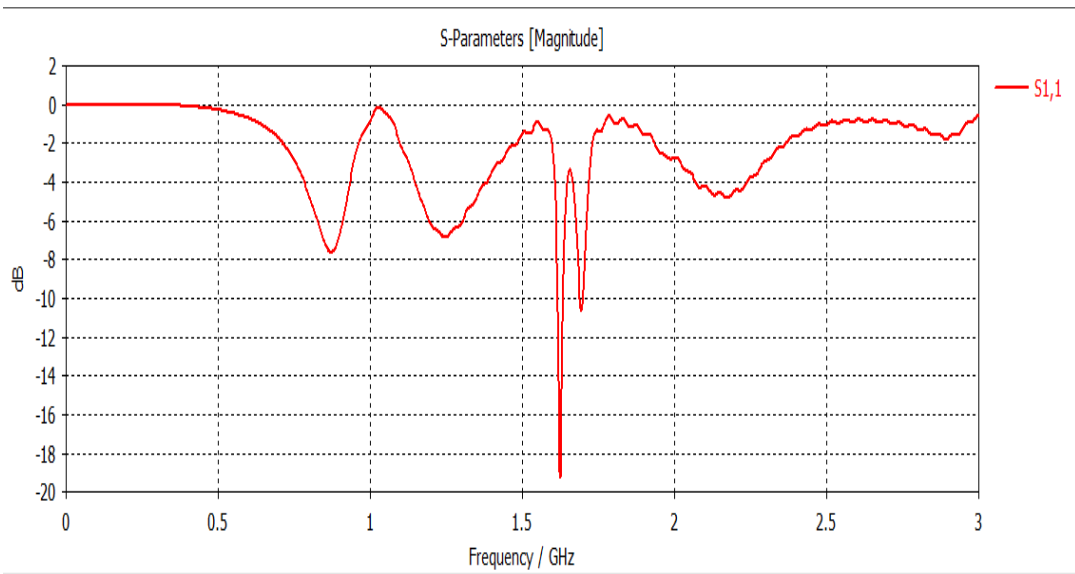


Figure 2.33 CST Design results of the bowtie antenna

The antenna yields the following 2D radiation patterns in the XY-plane:

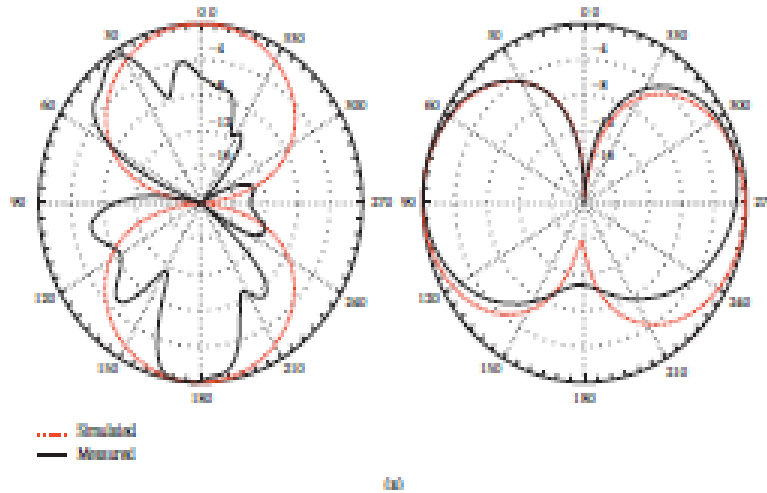


Figure 2.34 Radiation Patterns of the bowtie Antenna [16]

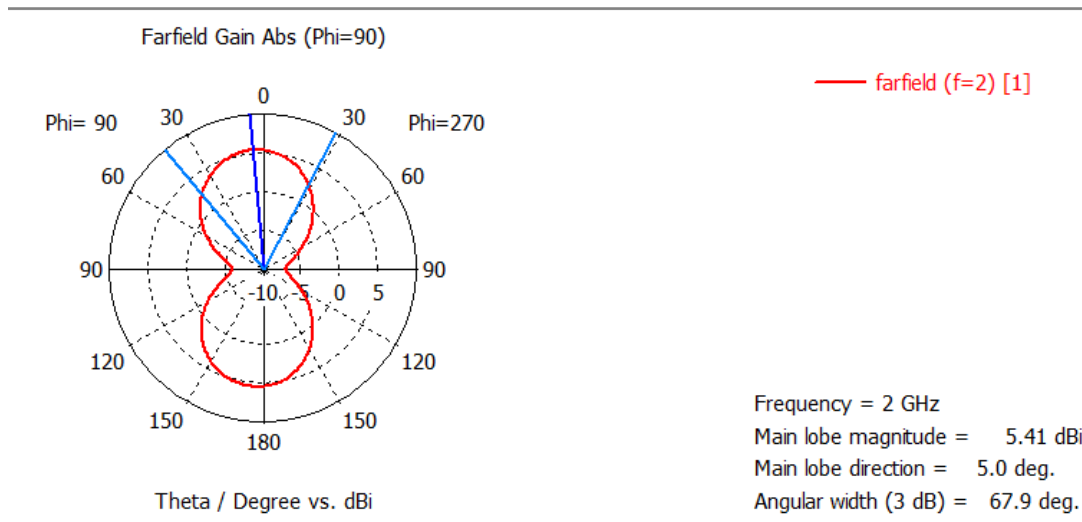


Figure 2.35 CST Design Radiation Pattern of bowtie antenna

2.5. Planar 3D Rectenna Array for Wireless Power Transfer Sensor Nodes

This work focused on making a 3D planar integrated Rectenna array for WPT and has a spherical DC coverage as well for empowering IoT sensor nodes. Previously, the Rectenna designs that were used for transmission and reception of power generally installed on the sidewalls and ceilings were only able to provide 2D coverage. This novel design proposes a 3D structure built in two-layer PCB technology for WPT and WEH systems. The design involves integration of tilted bore sight Rectenna and end fire Rectenna in azimuth plane and elevation plane. First, the two Rectennas are designed separately and key parameters are observed. The integration

includes six sectors of both the rectennas that offer insertion loss reduction and miniaturization. Boresight rectenna is designed using 3x1 patch antenna elements that also works as low pass filters [20]. The final product harvest 240Mv AT 1270 and 255Mv AT 1175 output. The whole rectenna array gives a single band output at 5.8GHz. Following is the rectenna designs and their implemented results.

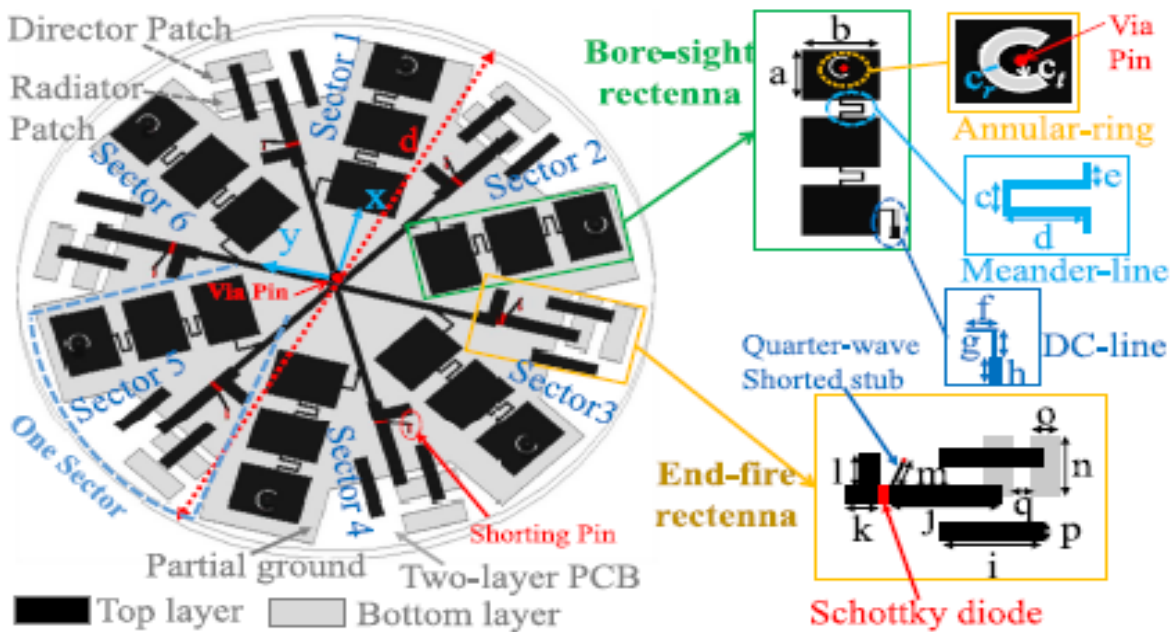


Figure 2.36 3D Radial Rectenna Array for RF Energy Harvesting [20]

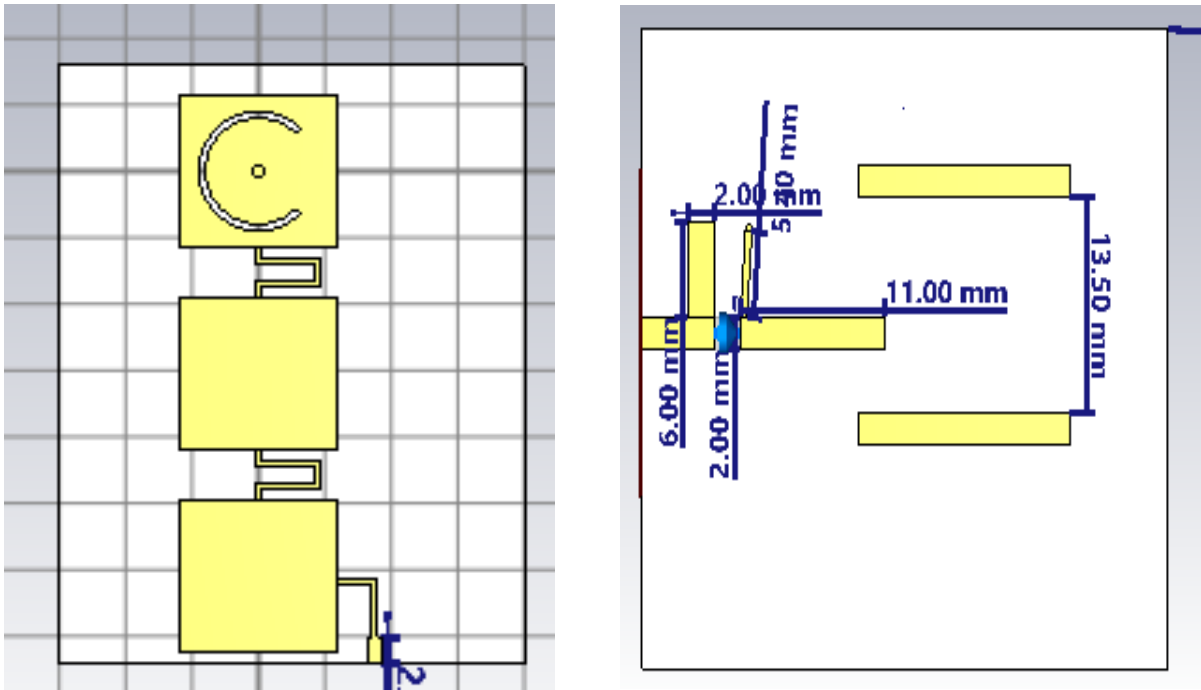


Figure 2.37 CST Design for (a) Bore sight Antenna (b) End fire Antenna
 The antenna yields a simulated result at single band of 5.8GHz.

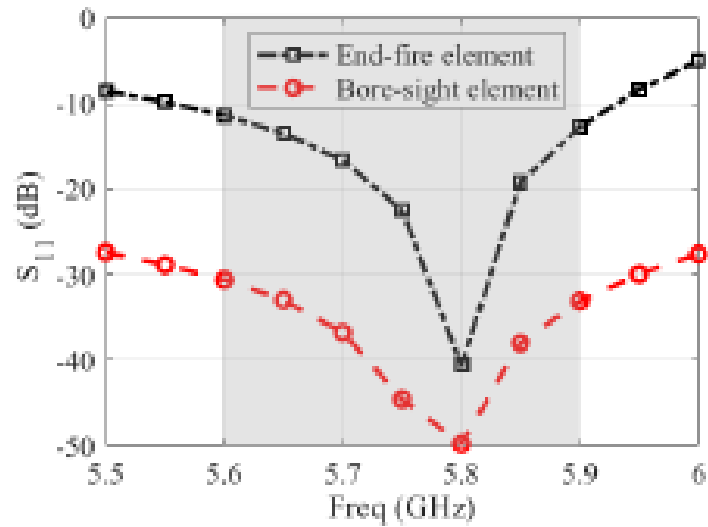


Figure 2.38 Return loss results for bore sight antenna and end fire antenna [20]

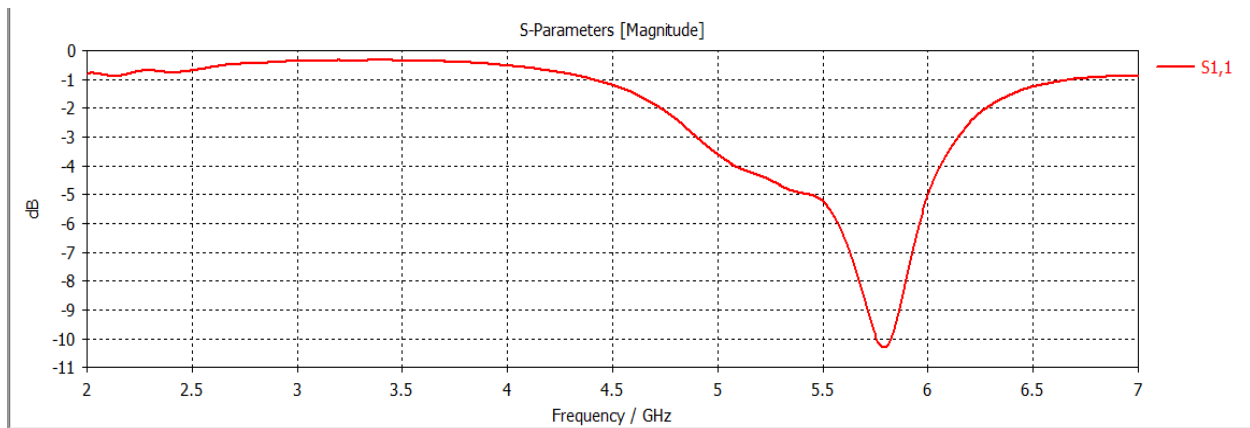


Figure 2.39 CST design results for bore sight and end fire antenna

The radiation patterns of the proposed Rectenna are as follows:

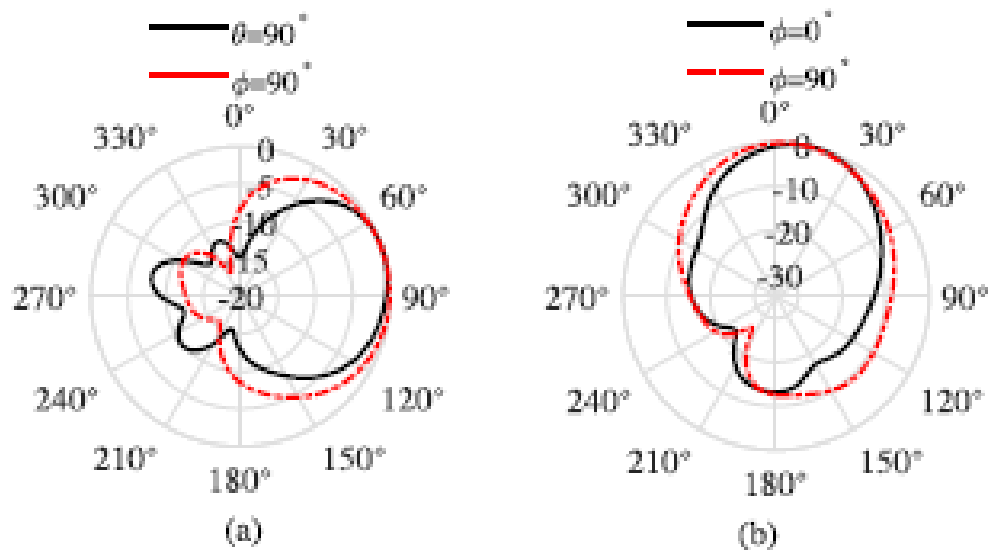
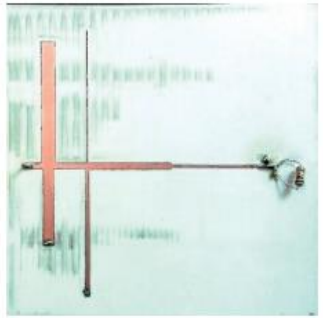

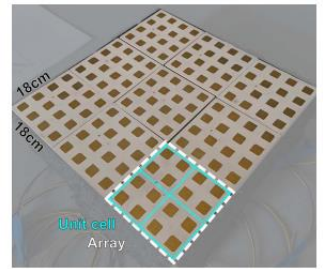
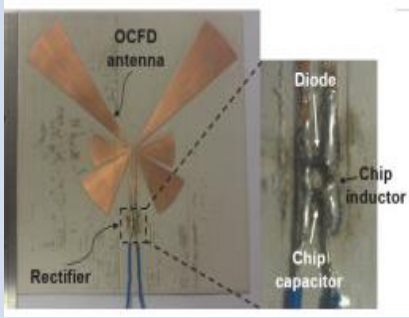
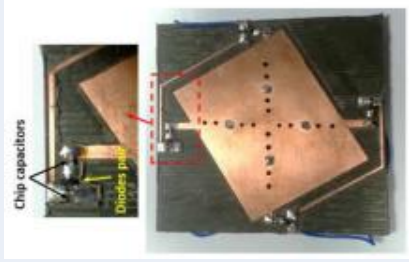
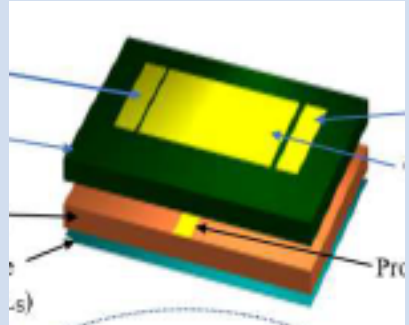


Figure 2.40 Radiation Patterns for Bore sight and End fire Antenna [20]

Here is a detailed literature review in tabular form.

2.6. Literature Review Table

Research Papers	Publication	Substrate	Operating Frequency	Antenna Efficiency	Size	Design
[1]. 3D Quad band Array Rectenna for Efficient Energy Harvesting	International Journal on Antennas and Propagation (2020)	FR4 substrate	98 MHz FM, GSM (900,1800), Wifi (2.4 GHz)	31.3% at -15dBm	10 × 10 × 10 cm ³ cube using FR4 substrate	
2. RF Energy Harvesting for Ubiquitous, Wireless Sensors	International Journal on Antennas and Propagation (2018)	Rogers Duroid 5880	0.5-2.4 GHz	67% at -5dBm	-	
3. Broadband RF Energy-Harvesting Arrays	IEEE Article (2022)	Rogers 4350B	10-GHz	30% above	-	

Research Papers	Publication	Substrate	Operating Frequency	Antenna Efficiency	Size	Design
4. Matching Network Elimination in Broadband Rectenna.	IEEE Transaction on Industrial Electronics (2016)	Rogers RT6002	0.9–1.1 GHz and 1.8–2.5 GHz	Above 60%	50mm	
5. Novel Compact and Broadband Frequency - Selectable Rectennas.	Journal Article (2018)	Rogers Duroid5880	1.1 to 2.7 GHz	Over 60% at (0-15dBm)	90 × 90 × 1.58 mm	
6. Microstrip Antenna for RF Energy Harvesting	CCPIS (2023)	FR4 & Rogers 5880	2.4 GHz	92%	80x60	

Chapter # 3

Research Methodology

In this chapter, the researcher will discuss different papers on proximity coupled antennas and their design mechanisms to confer how proximity coupled feeding technique is useful in designing a microstrip patch antenna and can result in improved bandwidth and overall efficiency of the antenna design. This will also give an insight to the student's understanding of this technique and her own research work.

3.1 An impedance matching method for broadband proximity coupled microstrip antenna

As discussed in chapter 1, feeding techniques are of two types. Contacting and Non-contacting. Proximity coupling comes under non-contacting technique in which a non-contact is made between feeding line and the radiator patch on the top of substrate. This results in greater bandwidth and increased efficiency in antenna. For this purpose, a standard dipole ground plane spacing is selected which gives critical coupling. This spacing gives maximum efficiency and bandwidth with respect to given height of feed layer. If the spacing is decreased, matching can still be achievable [21]. However, if the spacing is increased than it is difficult to achieve a match from the dipole to the feed line. This indicates that spacing is not effective to use as a parameter to broaden the antenna efficiency and bandwidth. In this regard, a lot of work has been done to improve the bandwidth of proximity coupling in microstrip antennas. For example appending parasitic radiator, inclusion of a matching network, L-probe feed, U-slot patch feeding, V-slot patch feed, Y-slot patch stub, tooth like slot patch, H-shaped slot in the ground plane etc. These methods can give antenna bandwidth from nearly 10% to 36%. So, a cavity is introduced in the ground plane. This reduces the surface waves that occur due to conventional cavities in the ground plane.

3.1.1. Design

In this work, a proximity coupled and cavity-backed microstrip antenna is proposed with a broadband impedance matching and wider efficiency. The narrow cavity is present to ensure essential coupling between the feed line and the radiator patch. A thicker substrate will be used increasing the coupling which will enhance the bandwidth. The design consists of two layers of

dielectric substrate. The dimensions of the patches are $W_x=7\text{mm}$ and $W_y=7\text{mm}$. The spacing between ground and the patch is $h=0.508\text{mm}$. The feed line width is $W_f=3\text{mm}$ which is centered with respect to the length of the cavity. The dimensions of the cavity with respect to the patch is $4 \times 8\text{mm}$ and thickness is 2mm . The design is made on Rogers 5880 substrate that has $\epsilon_r = 2.2$. Figure shows the design of the aforementioned antenna:

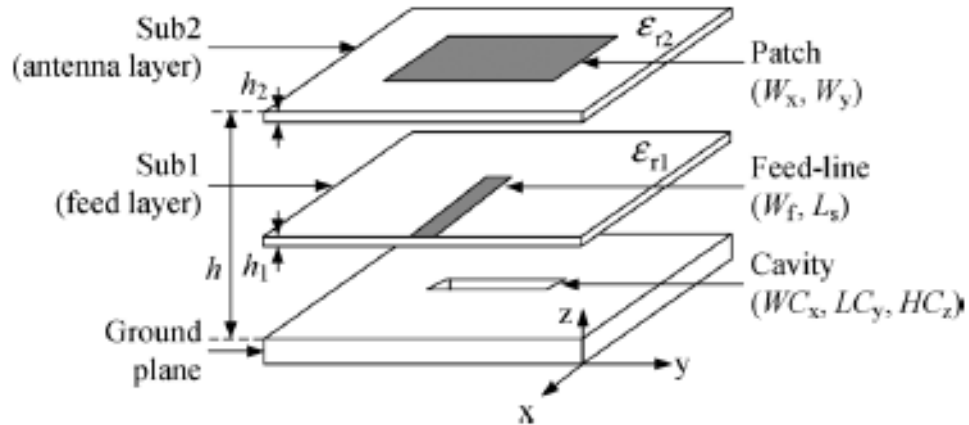


Figure 3.41 Antenna configuration [21]



Figure 3.42 Geometry of the cavity [21]

3.1.2. Result and Discussion

The voltage standing wave ratio (VSWR) of the design is shown in Fig. 2.2.

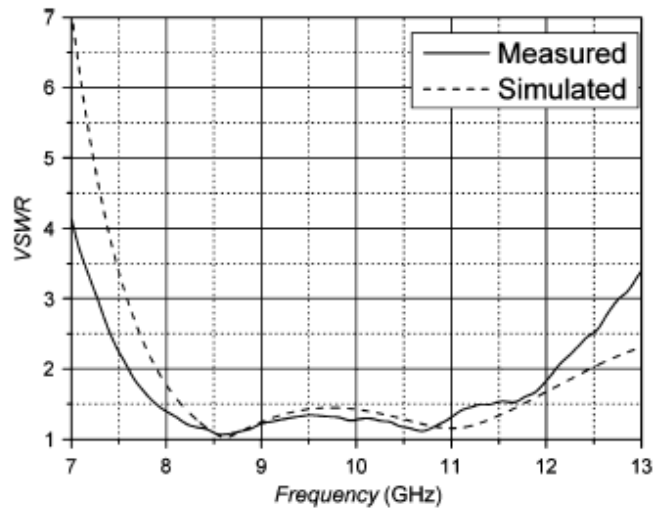


Figure 3.43 VSWR of cavity backed antenna [21]

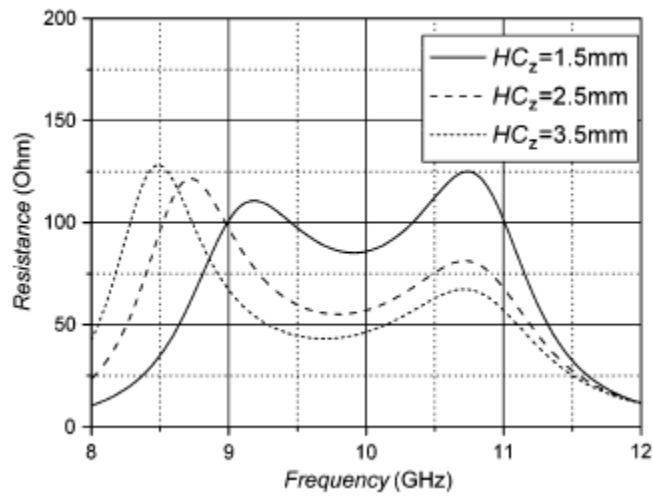


Figure 3.44 Antenna Input Impedance without cavity [21]

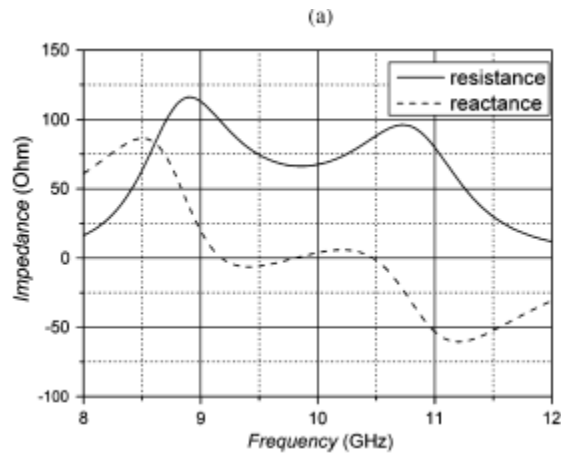


Figure 45 Antenna Input Impedance with cavity [21]

3.1.3. Conclusion

The cavity backed ground plane proximity coupled antenna is discussed above with the results. The design improves impedance matching and achieves critical coupling. A thicker substrate is used for laminating the design. The measured results has bandwidth over 40% which ensures the effective performance of the antenna.

3.2. A Dual-polarized Broadband Cavity backed Proximity-coupled Microstrip Antenna

In this research work, a broadband proximity coupled antenna is discussed here. The antenna has a ground plane which has a cavity and has standardized parameters which will enhance the coupling present at the feeding line and widen the bandwidth of the antenna. The design achieves less than -10dB bandwidth for more than 30% (8.2-11.4GHz) and the isolation between the port is greater than 20db which is covering the whole band [22]. The important part is this antenna is easy to fabricate and can be placed over a metal body for IoT application.

3.2.1. Design

The antenna design consists of a square patch with three dielectric substrates and two feed lines. The optimized cavity present at the ground plane gives good impedance matching and wider

Bandwidth. The substrates have a dielectric constant of $\epsilon_r = 2.2$ and heights of $h_1 = 1.575mm$, $h_2 = 3.175mm$ and $h_3 = 0.508mm$. The radiating patch is inserted between substrate 1 and 2 and has a size of $I_p \times I_p$ where $I_p = 6mm$. Here first substrate is acting as a dielectric layer, which will be used for further enhancing the overall bandwidth of the antenna. The orthogonal placement of feed lines between substrates 2 and 3, which are further connected to the inner conductor of coaxial probe. A narrow width cavity in the ground plane is designed to increase the coupling between radiator patch and the feed line, which will improve the impedance matching of the antenna. The cavity proposed here is L-shaped and the whole structure of the antenna is exactly symmetrical about the diagonal. Other parameters of the antenna are $I_c = 12.5mm$, $W_c = 4.3mm$, $h_c = 3mm$, $I_d = 2.75mm$, $W_d = 3.85mm$. In this design, the thickness of the proposed cavity is kept $h_c = 3mm$ which is quite smaller than quarter wavelength cavity design for the X-band applications.

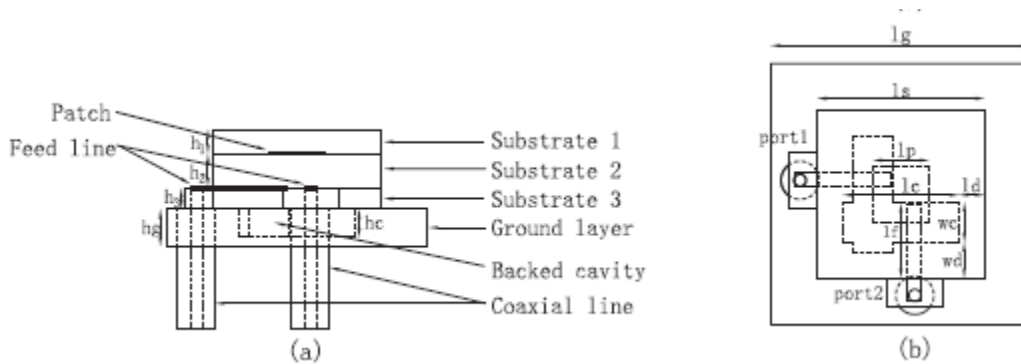


Figure 3.46 Cavity backed antenna with side view and top view [22]

3.2.2. Results and Discussions

As seen from the figure below, the design achieves a bandwidth of $<10Db$ for more than 30% (8.2-11.4) where as transmission loss is less $<20Db$ over the same bandwidth. This confirms that broad bandwidth can be achieved with dual polarized proximity coupled structure having L-shaped narrow cavity.

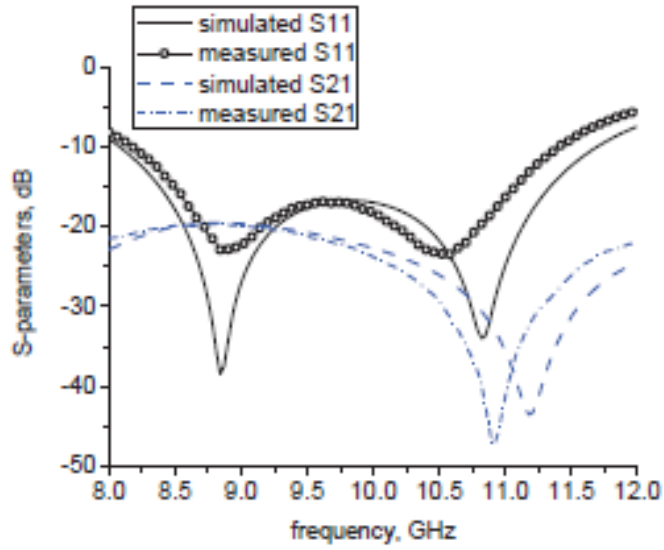


Figure 3.47 Simulation and measured result of the antenna [22]

To measure antenna radiation patterns, CST software is used and far-field setup is applied. The simulation results of E and H plane at 9.8GHz are attached below. It is evident that half power beam width (HPBW) in the co-polarization pattern in E-plane is about 85 and in the H-plane about 76.

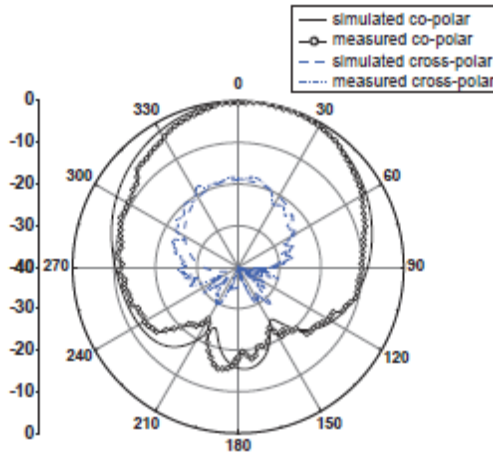


Figure 3.48 Simulated and Measured results of E-plane at 9.8GHz [22]

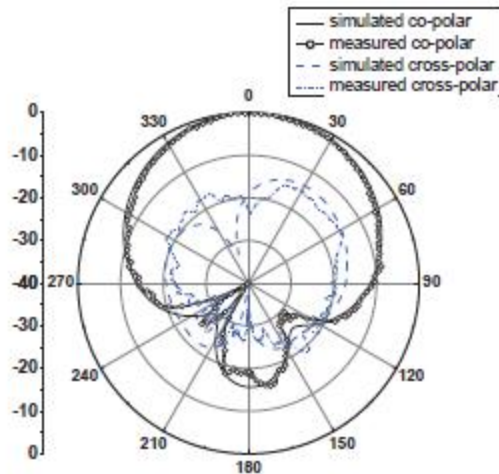


Figure 3.49 Simulation and Measurement results of H-plane at 9.8GHz [22]

3.2.3. Conclusion

A dual-polarized proximity coupled microstrip patch antenna is measured and simulated using CST software. The antenna has a optimizable cavity in the ground plane and achieves more than 30% bandwidth over 8.2-11.4GHz. The antenna shows stable radiation patterns in the E and H planes at 9.8GHz. The aforementioned design is easy to fabricate and can directly be mounted over the surface of the metal body. This confirms the antenna to be a good candidate for various applications.

3.3. Novel Broadband Proximity Coupled Microstrip Antenna Application for Conformal Phased Array Design

In this work, a broadband proximity coupled conformal phased array which has 49 linear arrays and four microstrip patch antennas is discussed. The antenna element has cavity backed ground plane and proximity coupling feed mechanism [23]. A dielectric substrate is designed to shield the antenna patches. This also plays an important role like that of a conformal radome. A vertical connection is designed between the coax probe and the feeding element which will enhance the space usage. The measured results are in good agreement with the simulated results and the antenna shows a maximum bandwidth of 27.6% with return loss below -10Db.

3.3.1. Design

The antenna design consists of three layers of dielectric substrates. A patch layer, a feed and a coaxial probe in the ground plane with a cavity. The parameters of three substrate layers are: $h_1 = 0.508mm$, $h_3 = 0.508mm$, $h_2 = 3.175mm$, $W_{px} = W_{py} = 6.2mm$, $W_x = 4mm$, $L_y = 10mm$, $\epsilon_{r1} = \epsilon_{r2} = \epsilon_{r3} = 2.2$. The upper patch size is $W_{px} \times W_{py}$. The antenna feed has width $W_f=3mm$. The feed line length is L_f . The cavity-backed ground and the patch on the top substrate is all aligned with respect to the center of the antenna. The cavity is slightly chipped from the edges in order to get the fabrication done easily. Here the cavity is responsible for the coupling between the layers and it can be adjusted easily. Moreover, the height of the substrate plays vital role in expanding the bandwidth of the antenna design.

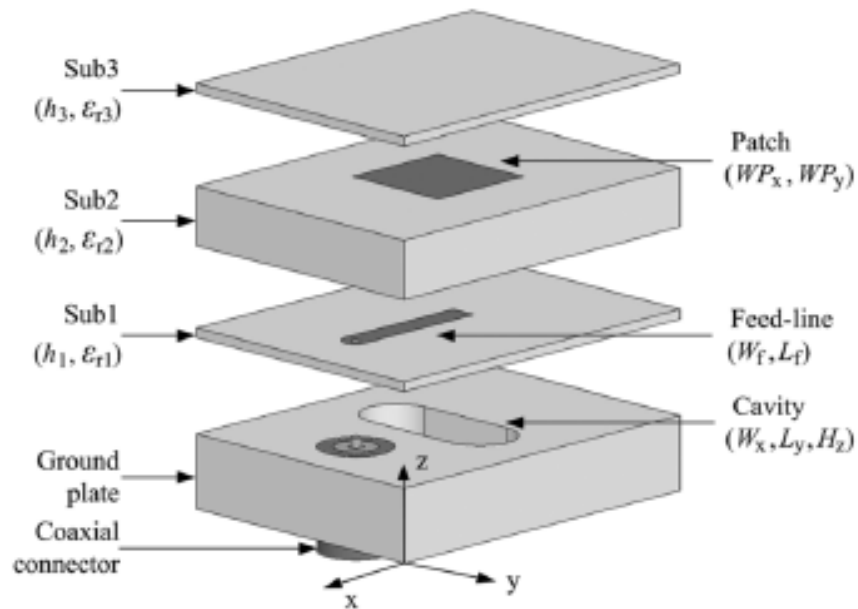


Figure 3.50 Structure of the proposed antenna [23]

3.3.2. Results and Discussions

The measured S11 of the proposed antenna is shown below:

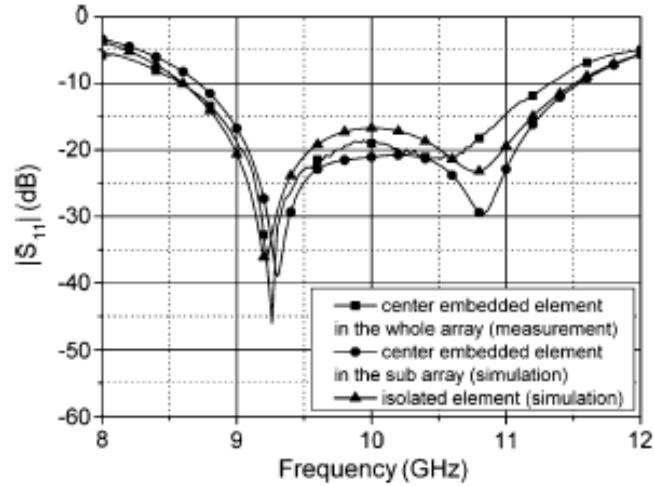


Figure 3.51 Results of the proposed antenna [23]

Here we can see that the antenna exhibits a bandwidth of 8.54GHz to 11.28GHz (27.6%). The antenna design shown above has been transformed into 48 sub arrays. The cross section has a sub radius of about 500mm and the central angle is 110. The 48 pieces are assembled piecewise due to extremely small size of one plane. These pieces are carved in a metallic frame shown in the figure below.



Figure 3.52 Prototype conformal phased array antenna [23]

3.3.3. Conclusion

The antenna design of a proximity coupled cavity backed microstrip antennas is discussed above. The coax probe design and its connection with the feed line is optimized to achieve a wide frequency band response and power transmission in different plane. The conformal phased array is based on the single unit antenna, which is realized because of via holes in the RF modules. This improves the reliability of the whole system. The substrate layer attached to the top of the antenna serves as a radome, which will further decrease the arrays volume.

3.4. Design of a antenna with a square backed cavity and dual polarization

In this work, a dual polarized microstrip patch antenna is designed using proximity coupling technique. The antenna has a cavity designed in square to increase coupling between the feed and the substrate and a good impedance bandwidth with isolation [24]. The proposed antenna has four feeds and they are coupled with the top patch electromagnetically. For high isolation two feed lines are excited out of phase between the ports. These type of antennas can be modeled for weather radar applications.

3.4.1. Design

This antenna design has three layers of substrates. The upper patch has a dielectric substrate layer. The middle layer has four feed lines with a feeding substrate. The bottom layer is a ground plane, which has a square cavity. The coaxial probe is vertically connected in the ground plane. The feeds are opposite to each other resulting in horizontal and vertical polarization. These feeds are vertically joined with the coax probe and have equal amplitude. The square patch on the top substrate is $W=5.72\text{mm}$ and $L=5.72\text{mm}$. The thickness of the top substrate is $h=3.175\text{mm}$ and $\epsilon_r = 2.2$. The feed lines present in the middle layer has width $W_f=1.01\text{mm}$ and length of the feed from the bottom of the antenna to the lamination open end is $L_f=1.52\text{mm}$. The height of feeding substrate is set to $h_f=0.508\text{mm}$.

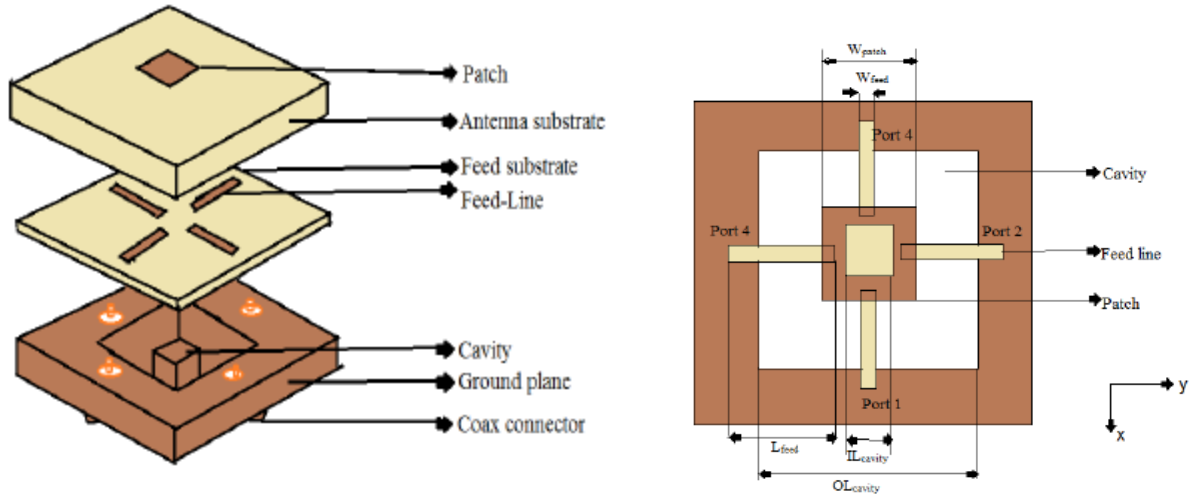


Figure 3.53 DP microstrip patch antenna structure [24]

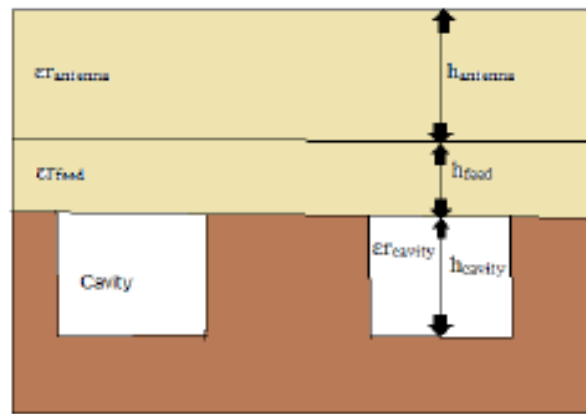


Figure 3.54 DP microstrip patch antenna structure (complete view) [24]

3.4.2. Results and Discussions

As shown above, a microstrip patch antenna is designed. The return loss and other radiation characteristics are obtained by giving appropriate excitation to the top patch. The antenna has four feeding lines. So, using dual polarized technique first two opposite feeding lines are excited and the other two are kept in off mode. This results in horizontal polarization. Next, these two feed lines, which were excited earlier, are kept in off mode and the other two feed lines are excited. This results in vertical polarization. Here, the total power obtained contains equal amplitude and are out of phase. The antenna gives a bandwidth of 2.5 MHz at 14.96GHz with the excitation of one port. When all four ports are excited simultaneously, the antenna exhibits 4

MHz bandwidth. It can be seen from the x-y plot that the bandwidth of the antenna is significantly increased using a DP (dual polarization) mechanism and a cavity backed ground plane.

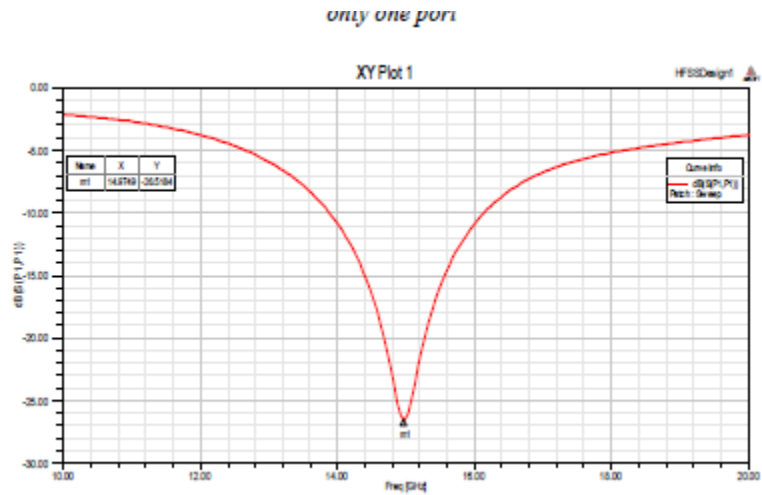


Figure 3.55 S11 plot for 1port [24]

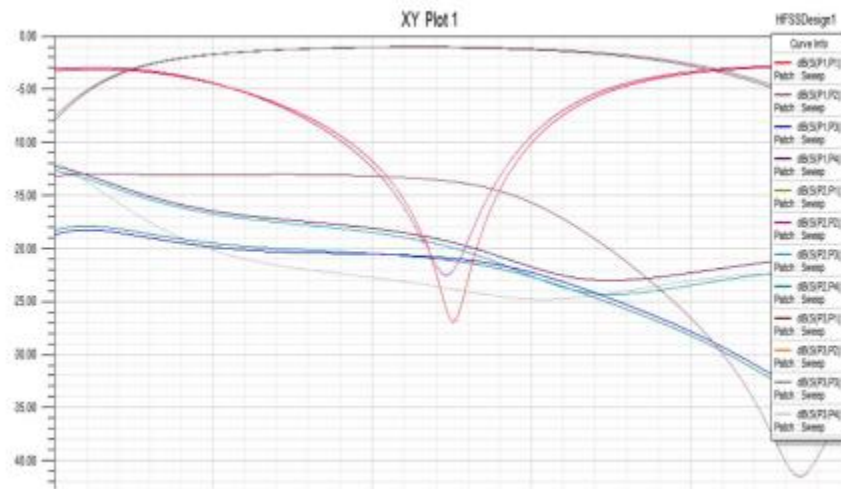


Figure 3.56 S11 plot for all four plots [24]

The pattern of the above design with one port and with all four ports.

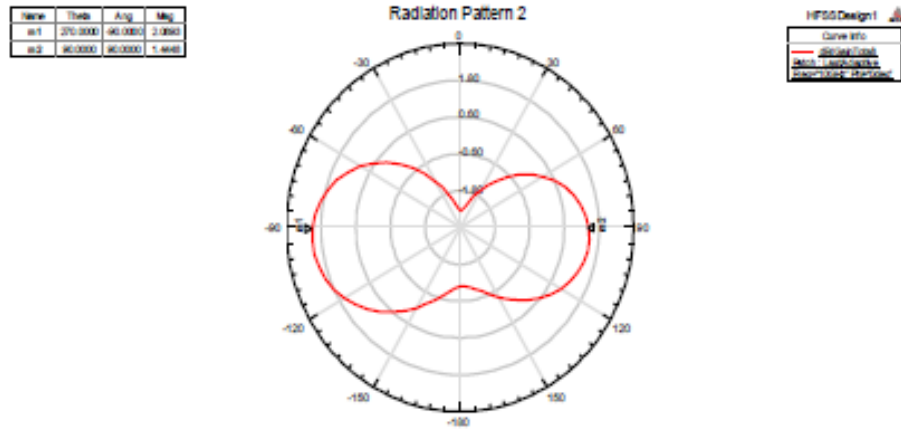


Figure 3.57 Radiation pattern plot for one port [24]

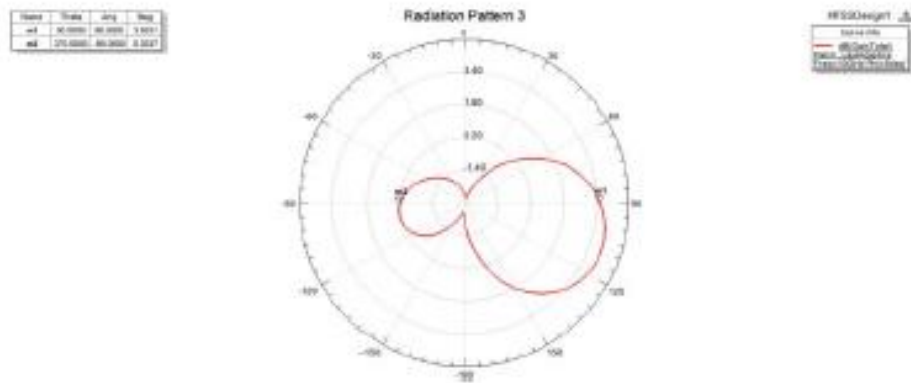


Figure 3.58 Radiation pattern for all four plots [24]

3.4.3. Conclusion

A proximity coupled microstrip patch antenna is presented with a square backed cavity. The antenna shows low cross polarization and increased bandwidth, which reduces inductances when probe feeding method is applied. These type of antennas are useful for weather radar applications and are easily fabricated.

Chapter # 04

Dual Band CP Microstrip Patch Antenna for RF Energy Harvesting

In this chapter, the design evolution to achieve dual band circularly polarized microstrip patch antenna is presented and the results are discussed in detail. The researcher aims to realize the antenna using proximity coupled feeding technique. The final antenna design along with its fabricated prototype is shown in the subsequent sections. The cavity backed coax feeding is crucial to realize the results in this regard.

4.1. Introduction

In the dynamic landscape of wireless communication systems, antennas play an important role in verifying the efficient and reliable transmission of signals. Proximity-coupled antennas have emerged as a groundbreaking phenomenon in antenna design, providing excellent advantages in terms of performance, fabrication, and the ability to be scaled down. Unlike conventional antennas, which often depend on direct electrical connections, proximity-coupled antennas involves the use of electromagnetic coupling to achieve better functionality.

The concept of proximity coupling requires placing electrical components in close proximity without direct physical contact, resulting in improved impedance matching, broader bandwidth, and reduced interference. This innovative approach has gained significant attention across various applications, ranging from wireless communication devices to sensor networks and beyond.

A key advantage of proximity-coupled antennas lies in their ability to attain compact and remarkable designs, making them particularly suitable for environments with space constraints and for modern electronic devices where size and form factor are a matter of concern. Additionally, these antennas highlight multitasking in terms of frequency variations, enabling seamless adaptation to different communication standards and frequency bands.

This introduction aims to offer an insight into the domain of proximity-coupled antennas, diving into the fundamental principles governing their operation, the advantages they bring, and the

diverse applications that can be obtained on their unique capabilities. As the antenna design is evolved further and the complexities it involves, it becomes evident that proximity coupling signifies a paramount transfer in antenna design engineering, which reveals possibilities for enhancing wireless communication systems in our increasingly interconnected world.

4.2 Design Evolution

After spending brief time learning and understanding the concept, visualization and technique behind proximity coupling, a stacked microstrip patch antenna is designed. Initially a simple microstrip patch antenna is designed and then stacking is introduced in the top to obtain the results at the required frequency bands. Lastly, a cavity is introduced in the ground to improve the bandwidth of the antenna and coupling between the dielectric layers. The final design performs at GSM 1.8GHz and Wi-Fi2.4GHz and is circularly polarized. The aforementioned antenna is depicted in the Figure 4.59.

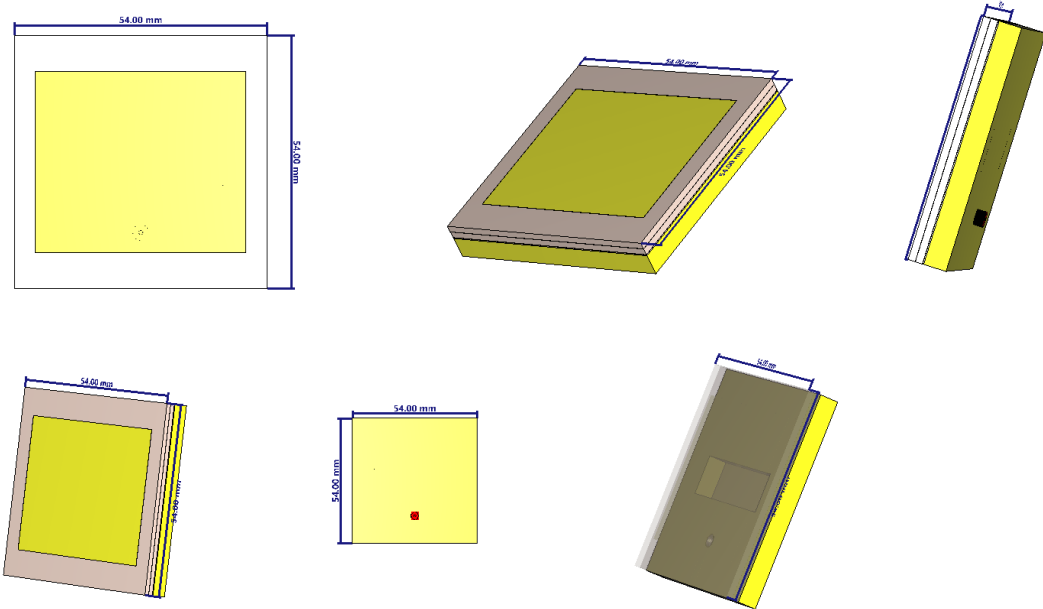


Figure 4.59 Proximity Coupled Stacked Patch Antenna

4.2.1. Simulated Results:

The design yields antenna efficiency of 60% and 95% at 1.8GHz and 2.4GHz respectively. This design is completed using Rogers 5880 with $\epsilon_r = 2.2$ and thickness 3.175mm for the upper patch and 2.54mm thick Rogers 5880 for the lower patch. The feeding substrate has dielectric constant of 2.2 and is 0.254mm thick. The cavity present in the ground is 40x10mm and is centered with respect to y-axis. The feed line placed at the top of feeding substrate surpasses the cavity present in the ground by 35mm length. The feed width is 3mm. After simulation, antenna gives the return loss in Figure 4.60:

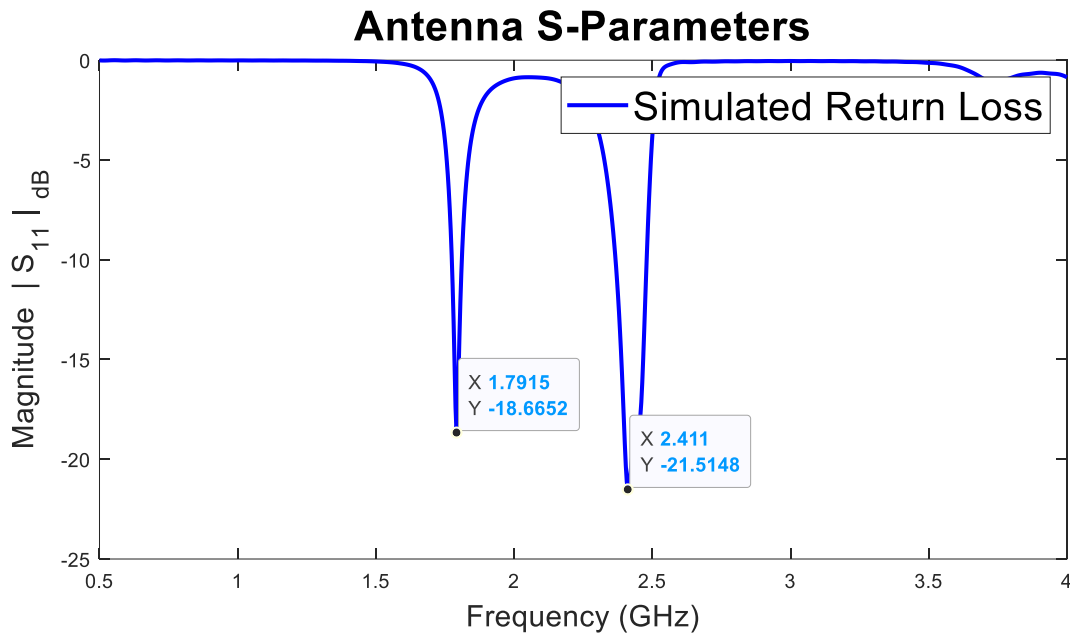


Figure 4.60 S11 of the stacked microstrip patch antenna

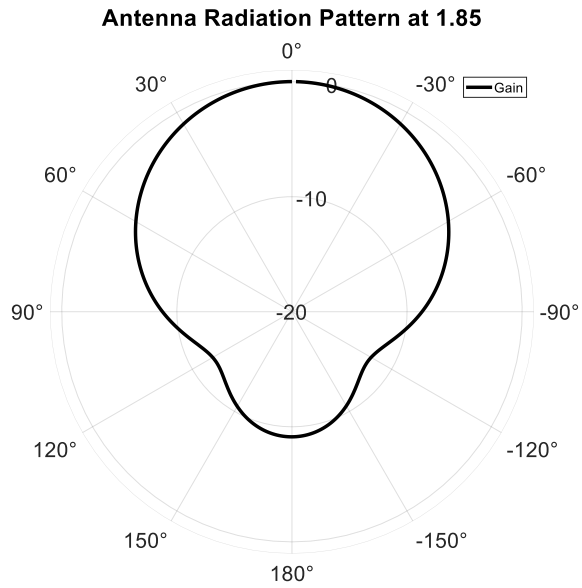


Figure 4.61 Radiation Pattern at 1.8GHz

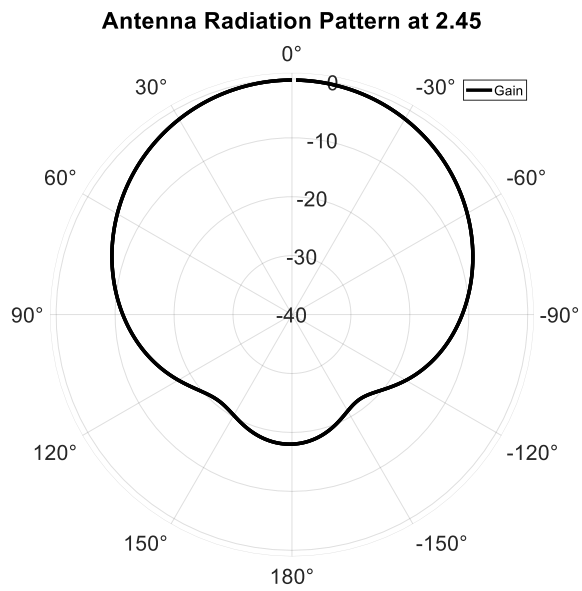


Figure 4.62 Radiation Pattern at 2.4GHz

Here is the 3D radiation pattern of the antenna at 1.8 GHz with gain of 5.2dBi:

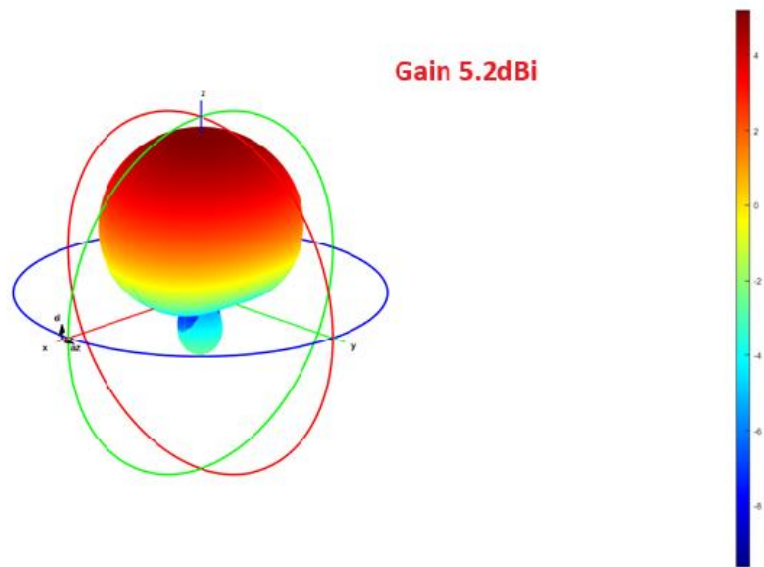


Figure 4.63 3D Radiation Pattern at 1.8GHz (5880)

And this is 3D radiation pattern of the antenna at 2.4 GHz with gain of 5.85dBi:

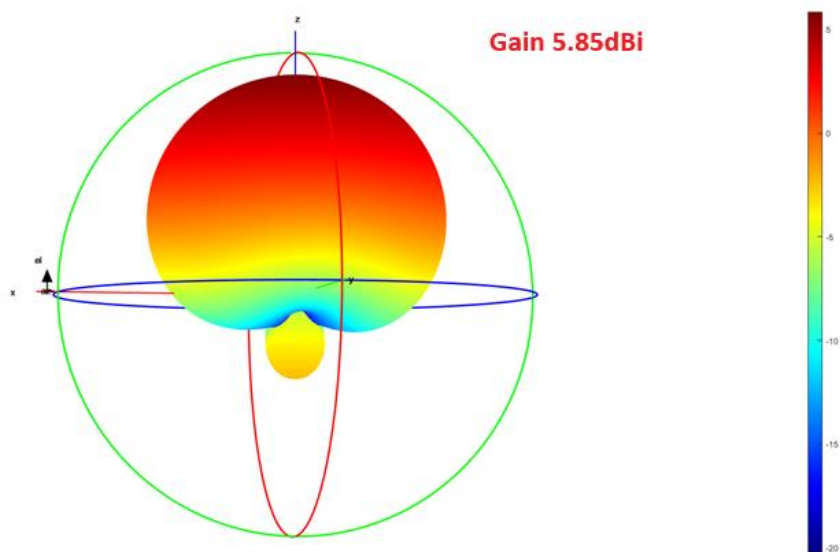


Figure 4.64 3D Radiation Pattern at 2.4GHz (5880)

The antenna shows radiation efficiency of 96% and 95% at 1.8GHz and 2.4GHz respectively.

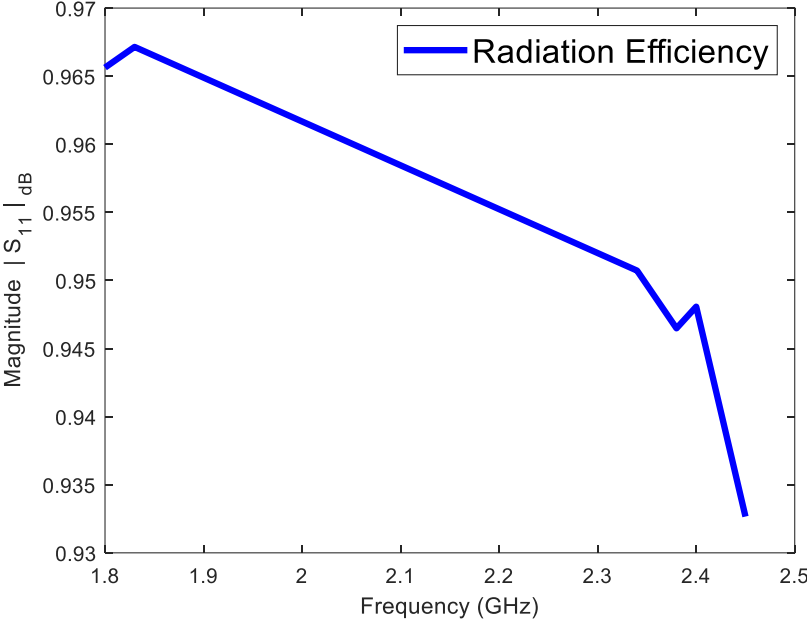


Figure 4.65 Antenna Radiation Efficiency

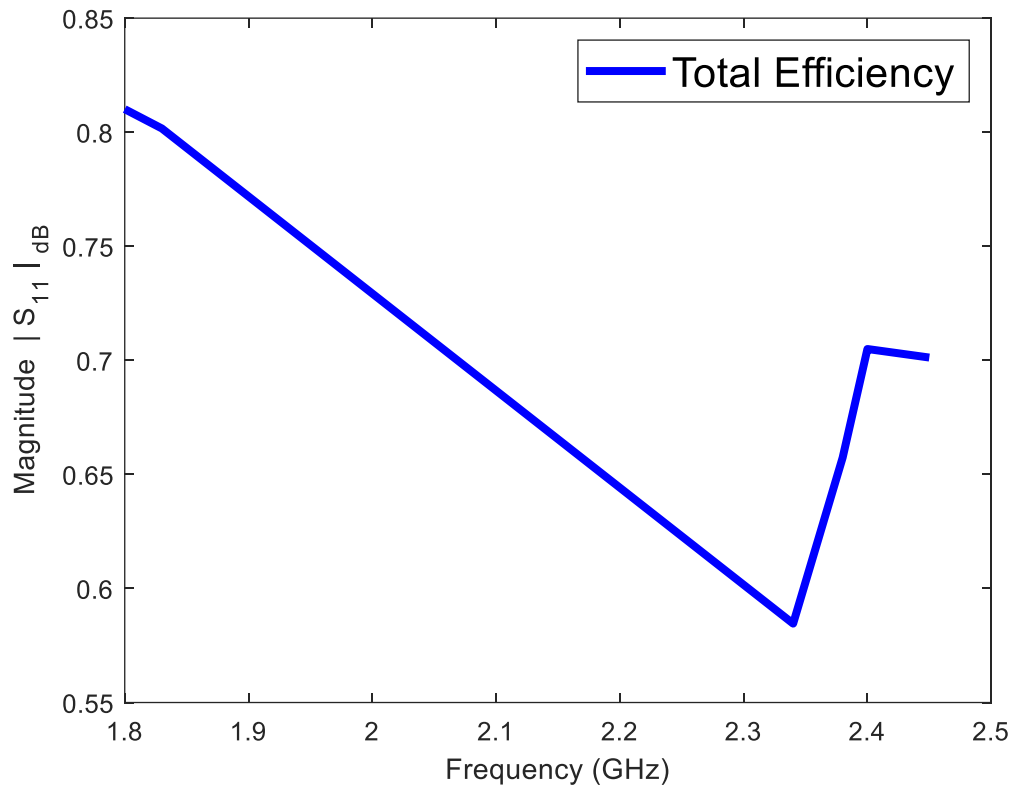


Figure 4.66 Antenna Total Efficiency

The total efficiency is 80% and 60% respectively.

4.3. Design Challenges

Now, when it comes to realization, the difficult part was to find Rogers 5880 substrate with the thickness on which it was designed. Interestingly, this thickness was not commercially available. So, to make things simpler the same design was converted to Rogers 5880 with the thickness 1.57mm which is commercially available and is also present in the data sheet. The upper substrate was changed to Rogers 5880 and the lower substrate was changed to Rogers 5870. When the upper substrate dielectric thickness was changed, the results were entirely different. It is therefore mention that the cavity present in the ground and the feed line was then optimized to get the same results at these two frequency bands. The return loss came out is shown in Figure 4.67:

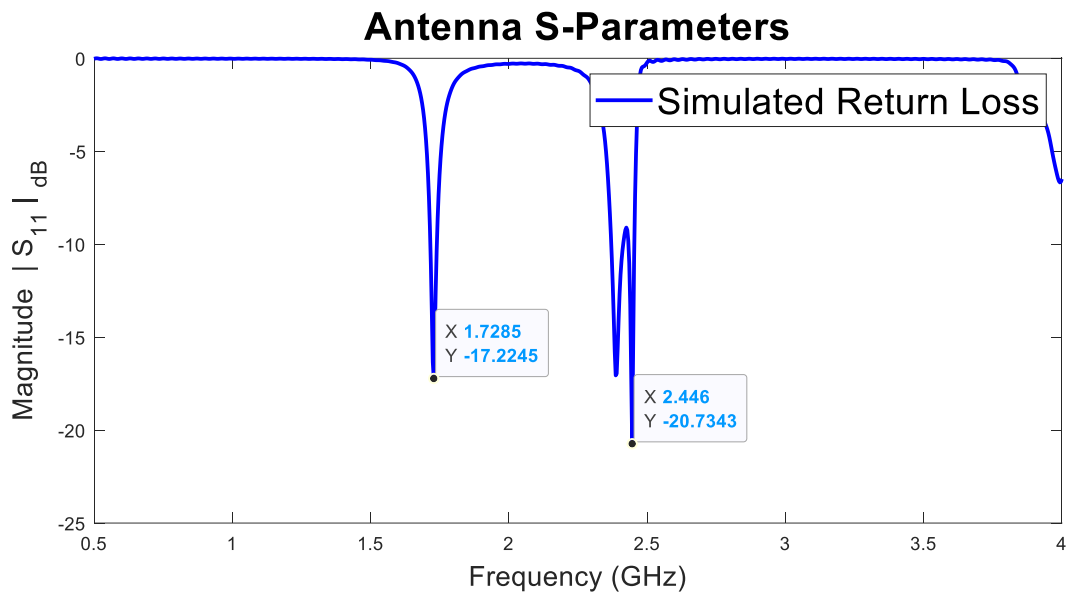


Figure 4.67 S11 of the stacked microstrip patch antenna (substrate 5880)

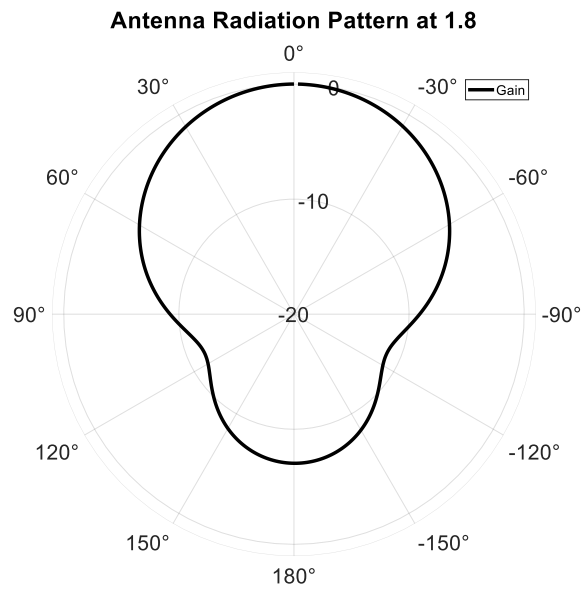


Figure 4.68 Antenna Radiation Pattern at 1.8GHz

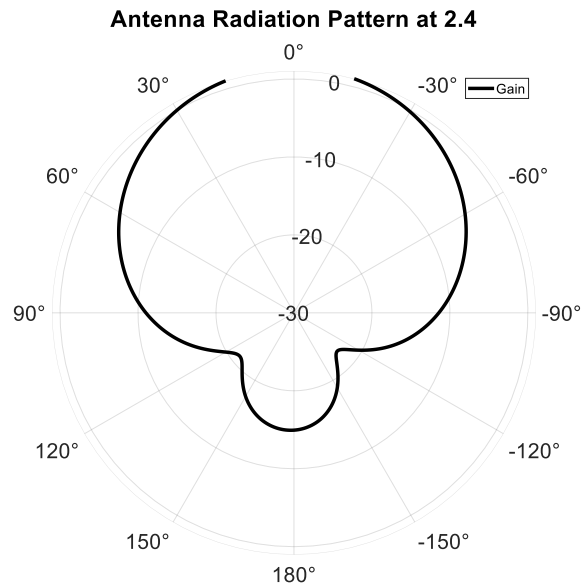


Figure 4.69 Antenna Radiation Pattern at 2.4GHz

But given the circumstances and less resources at hand, the design was again converted to Rogers 5870 with $\epsilon_r = 2.33$ and thickness $1.57mm$ for both the upper and lower substrate. The feeding substrate was kept Rogers 5880 with thickness $0.254mm$. This time, slight changes occurred in terms of return loss and overall antenna radiation characteristics due to minor difference between the values of both dielectric substrates. Here is the return loss that came out afterwards shown in Figure 4.70:

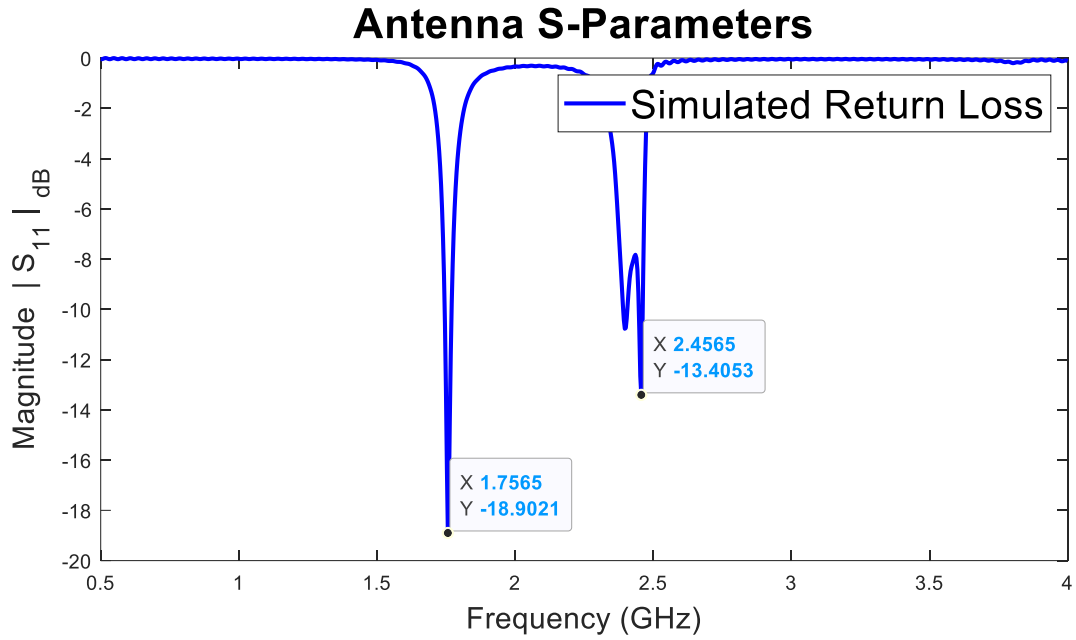


Figure 4.70 S11 of the stacked microstrip patch antenna (substrate 5870)

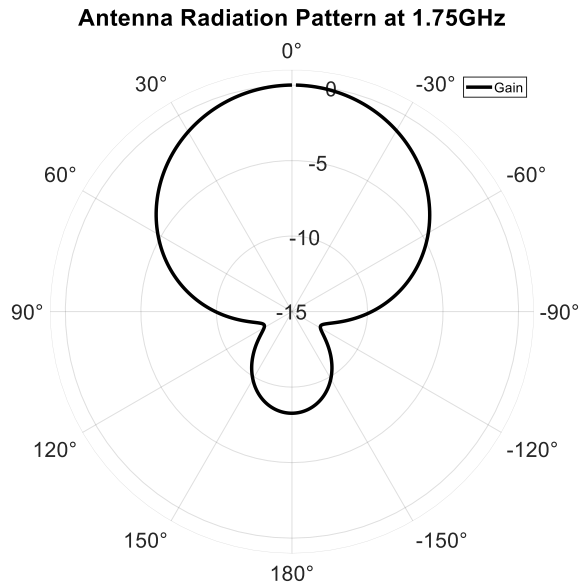


Figure 4.71 Antenna Radiation Pattern at 1.8GHz

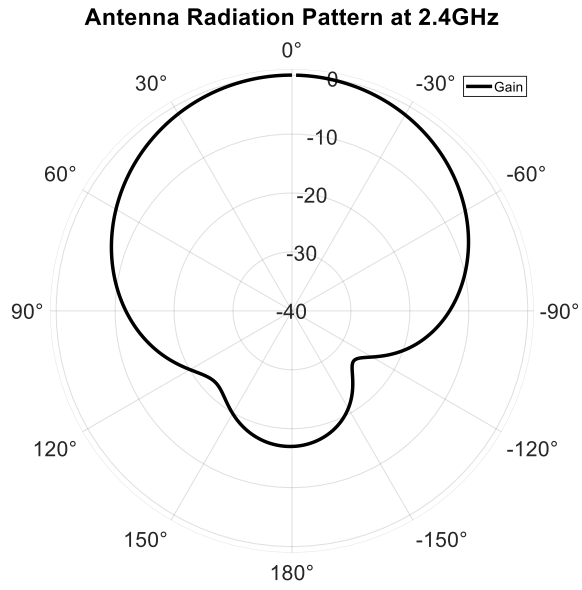


Figure 4.72 Antenna Radiation Pattern at 2.4GHz

Here is the 3D radiation pattern of antenna at 1.8 GHz with gain of 5.12dBi:

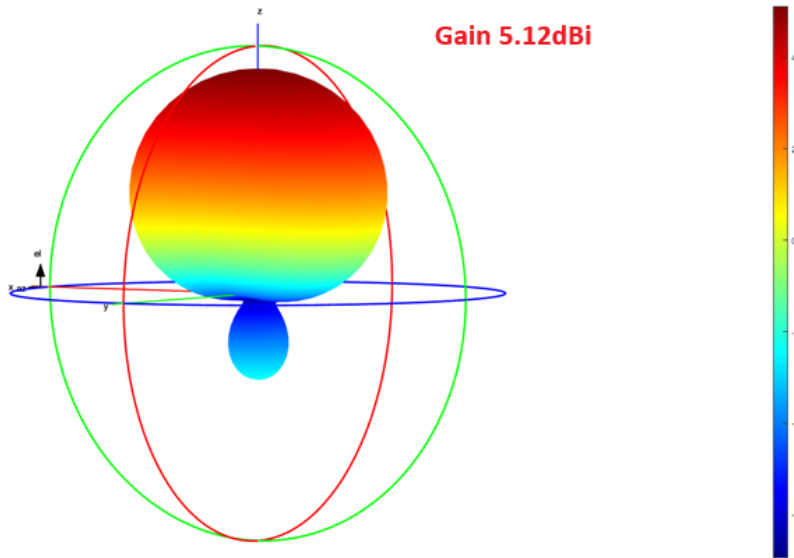


Figure 4.73 3D Radiation Pattern at 1.8 GHz (5870)

Here is the 3D radiation pattern of antenna at 2.4GHz with gain of 5.12dBi:

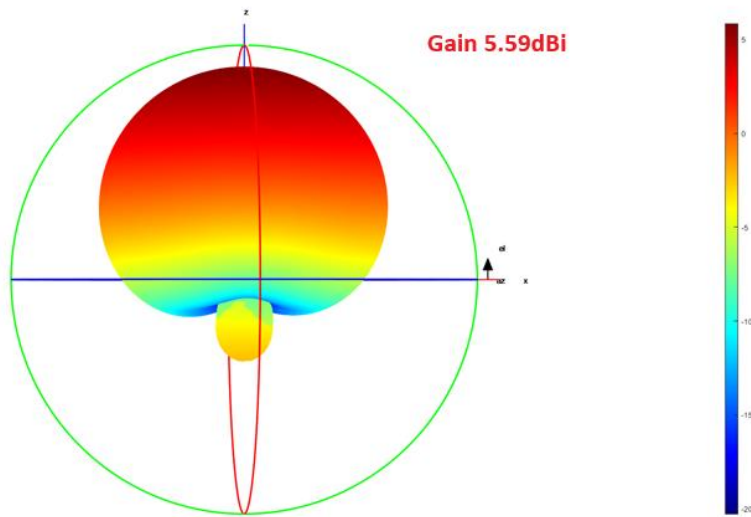


Figure 4.74 3D Radiation Pattern at 2.4GHz (5870)

The antenna shows radiation efficiency of 90% and 76% at 1.8 and 2.4 GHz respectively.

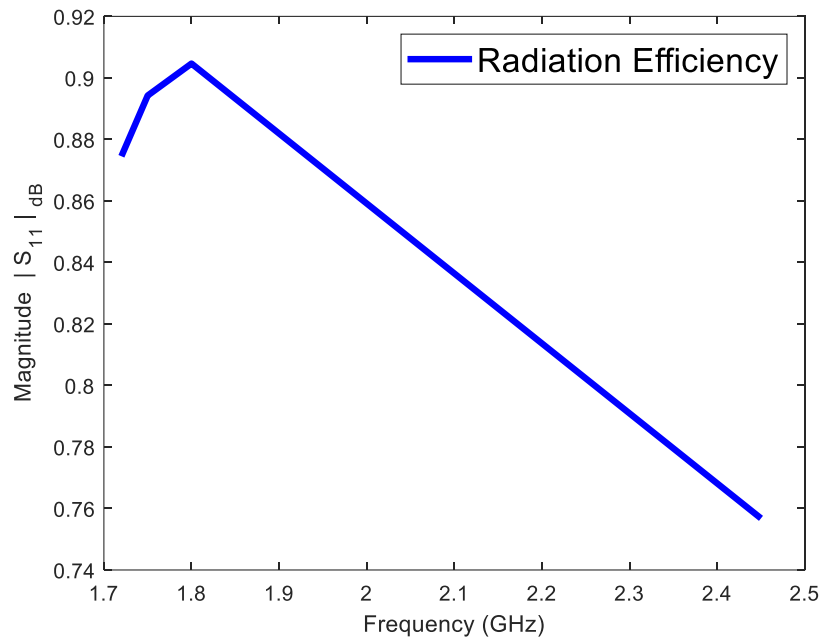


Figure 4.75 Antenna Radiation Efficiency (5870)

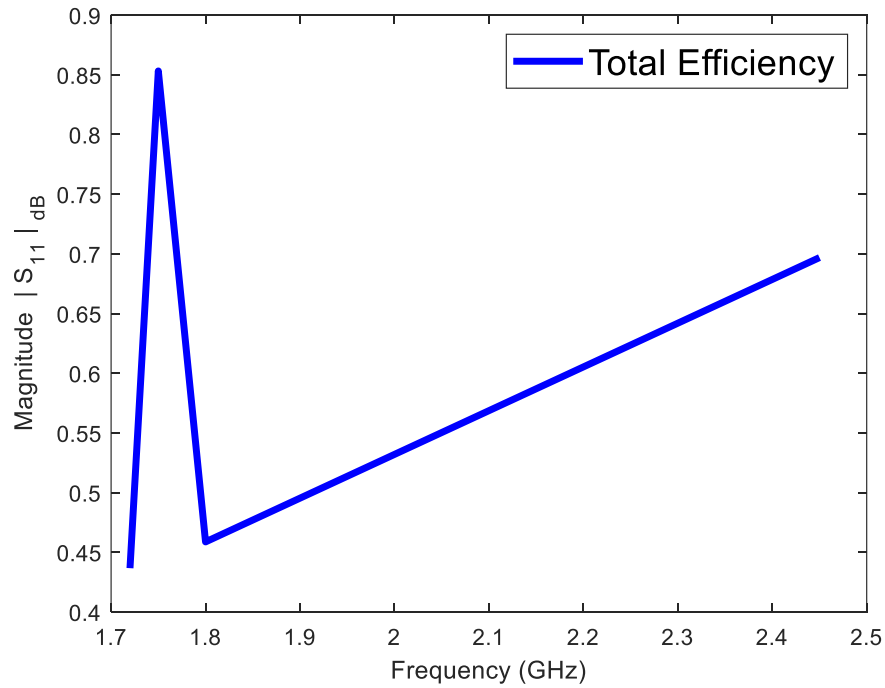


Figure 4.76 Antenna Total Efficiency (5870)

4.2.3. Coax Connection

After the design was simulated using waveguide port applied on the feed line and desired results were achieved, the need to visualize the antenna results after fabrication arises. So, a coax connection was made in the ground with inner coax touching the feed line and outer coax touching the ground. In between, a thick insulator was also placed as shown in Figure 4.77. This coax connection plays a significant role in optimizing the results. The pin of the inner coax is kept 0.9mm and that of outer coax 3mm. It is due to the dimensions available commercially for SMA connectors. The location of this coax probe is important as it is placed below the cavity in the ground.

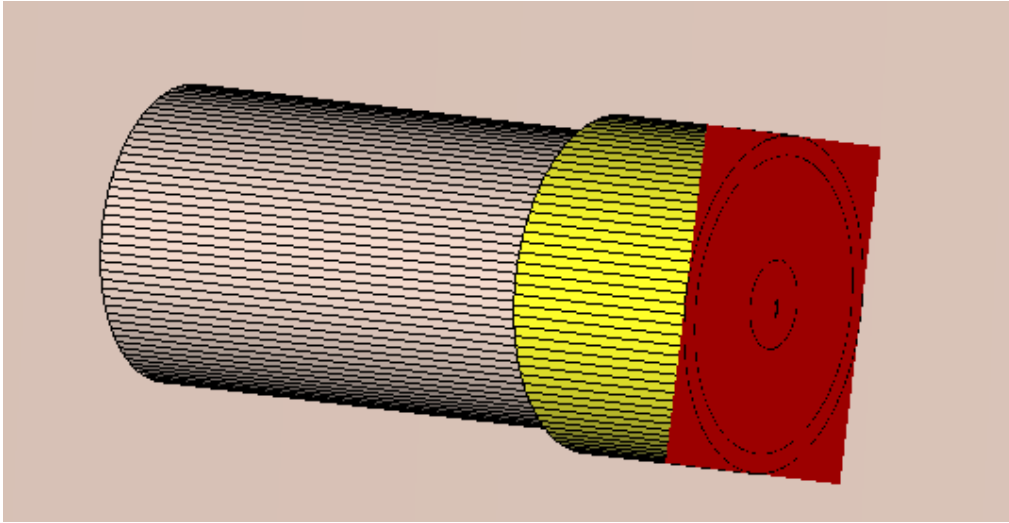


Figure 4.77 Coax Connection

4.2.4. Circular Polarization

In order to make the above designed antenna circularly polarized, a number of papers were read and finally one technique is applied in which a corner of the upper patch is cut thereby reducing the phase difference [31]. For CP, axial ratio is the key factor that determines the polarization of the antenna. This factor should be 3dB or less in this regard. In the figure shown below, a 7.6mm patch is cut from the upper patch of the designed antenna which is shown in Figure 4.78:

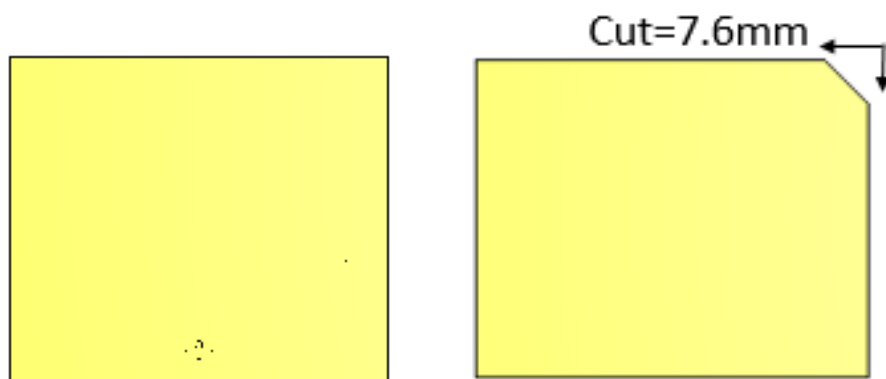


Figure 4.78 Antenna (LP) vs. Antenna (CP)

Here the axial ratio comes out to be:

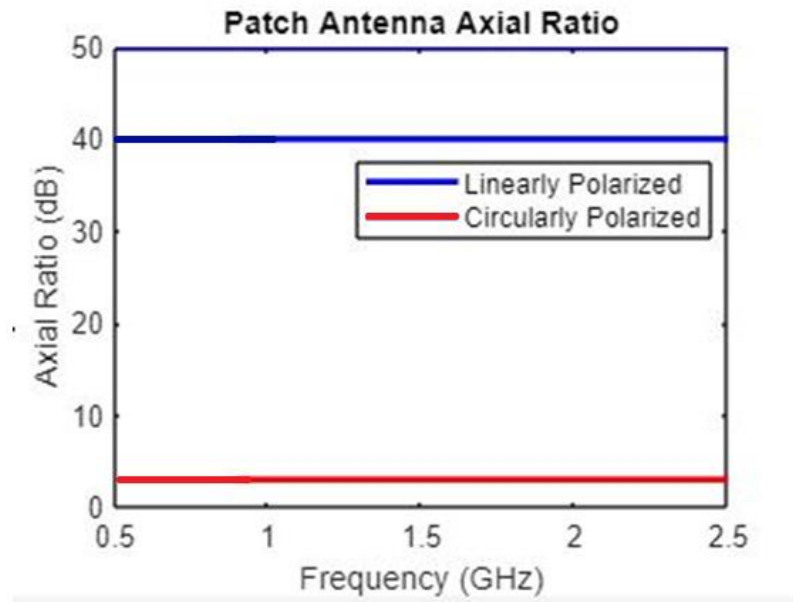


Figure 4.79 Patch Antenna Axial Ratio

4.2.5. Fabricated Prototype

Image below shows the fabricated antenna, in which the substrate layers were fabricated using LPFK machine present in RIMMS prototype lab. The cavity-backed coax installed ground was manufactured using CNC machine. The assembling of both the substrate layers and antenna ground was done in RIMMS and its testing was completed in the anechoic chamber located at RIMMS, NUST.

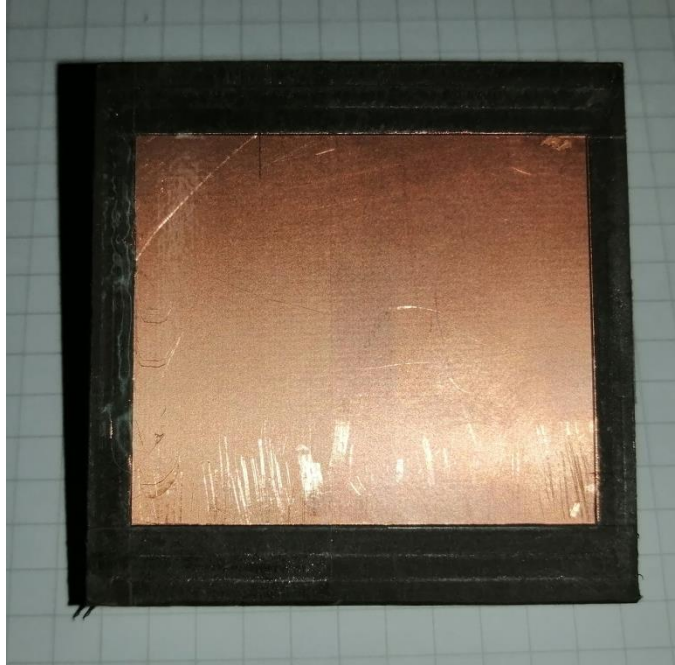


Figure 4.80 Fabricated Antenna (Front)

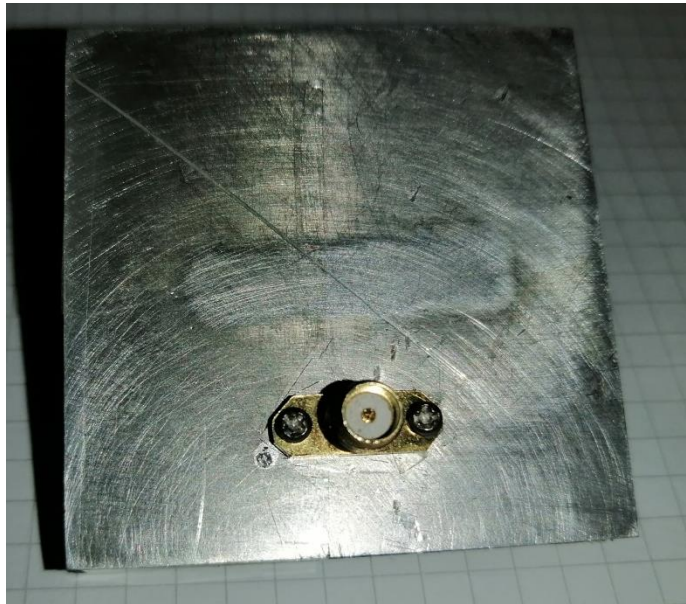


Figure 4.81 Fabricated Antenna (back)

4.2.6. Measured Results

The testing of the above designed antenna was performed in the anechoic chamber located in the RIMMS, NUST.



Figure 4.82 Antenna shorting Test



Figure 4.83 Antenna placed in the anechoic chamber

The antenna return loss came out as shown in Figure 4.84.

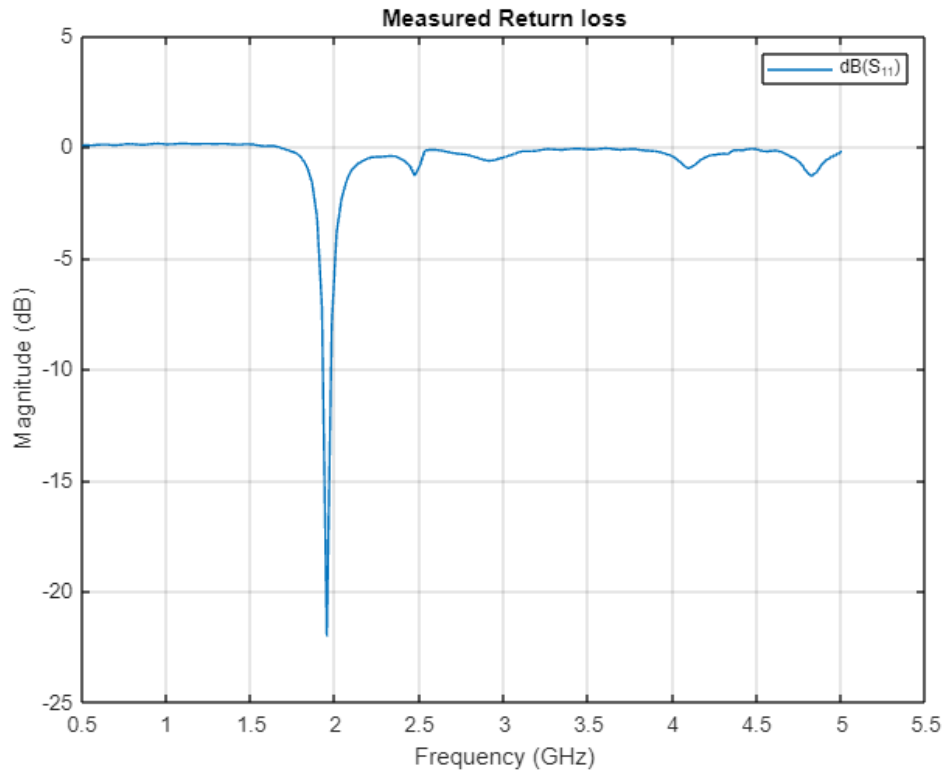


Figure 4.84 Measured return loss of stacked proximity coupled antenna

4.2.7. Radiation Patterns

The designed antenna was placed in the anechoic chamber for testing. The antenna was able to perform on the desired frequency bands with following gain in the azimuth and elevation planes:

4.2.7.1. Azimuth Plane

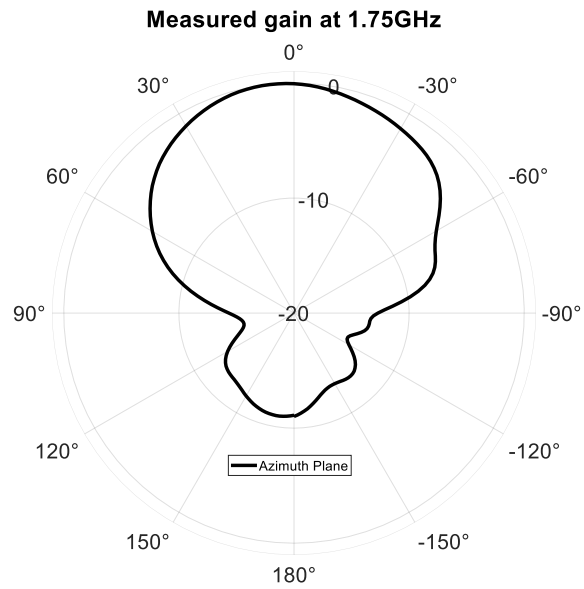


Figure 4.85 Measured gain in the azimuth plane(1.75ghZ)

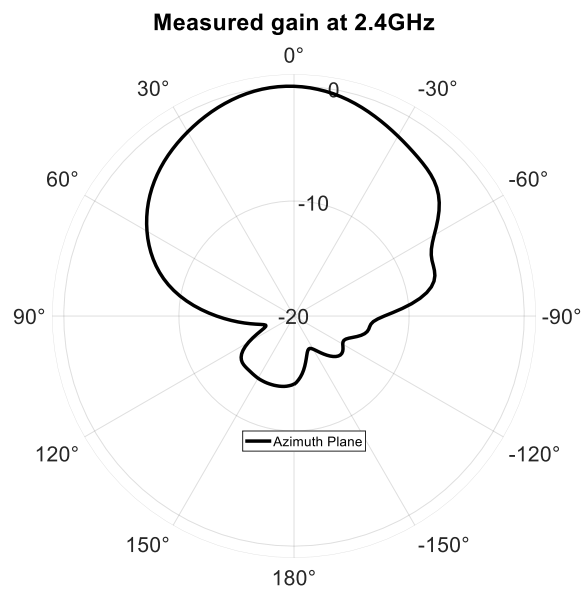


Figure 4.86 Measured gain in the azimuth plane (2.4ghZ)

4.2.7.2. Elevation Plane

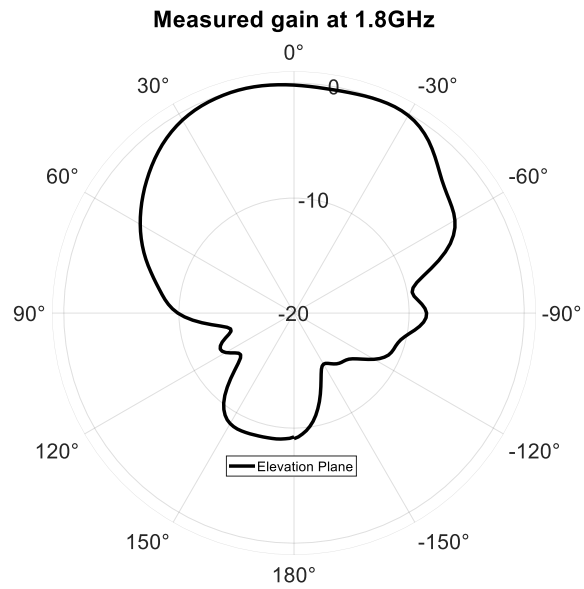


Figure 4.87 Measured gain in the elevation plane(1.75ghZ)

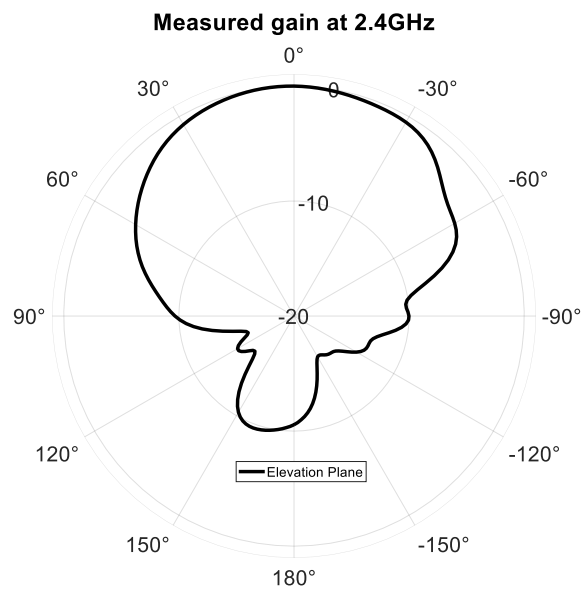


Figure 4.88 Measured gain in the elevation plane (2.4ghZ)

4.2.8. Results Comparison

In the end a result comparison is performed by taking into account both the simulated and measured results side by side. The comparison is performed using MATLAB and is shown below. It is pertinent to note that return loss of the measured results is slightly shifted meanwhile the radiation patterns come nearly close to simulation results after measuring in the anechoic chamber.

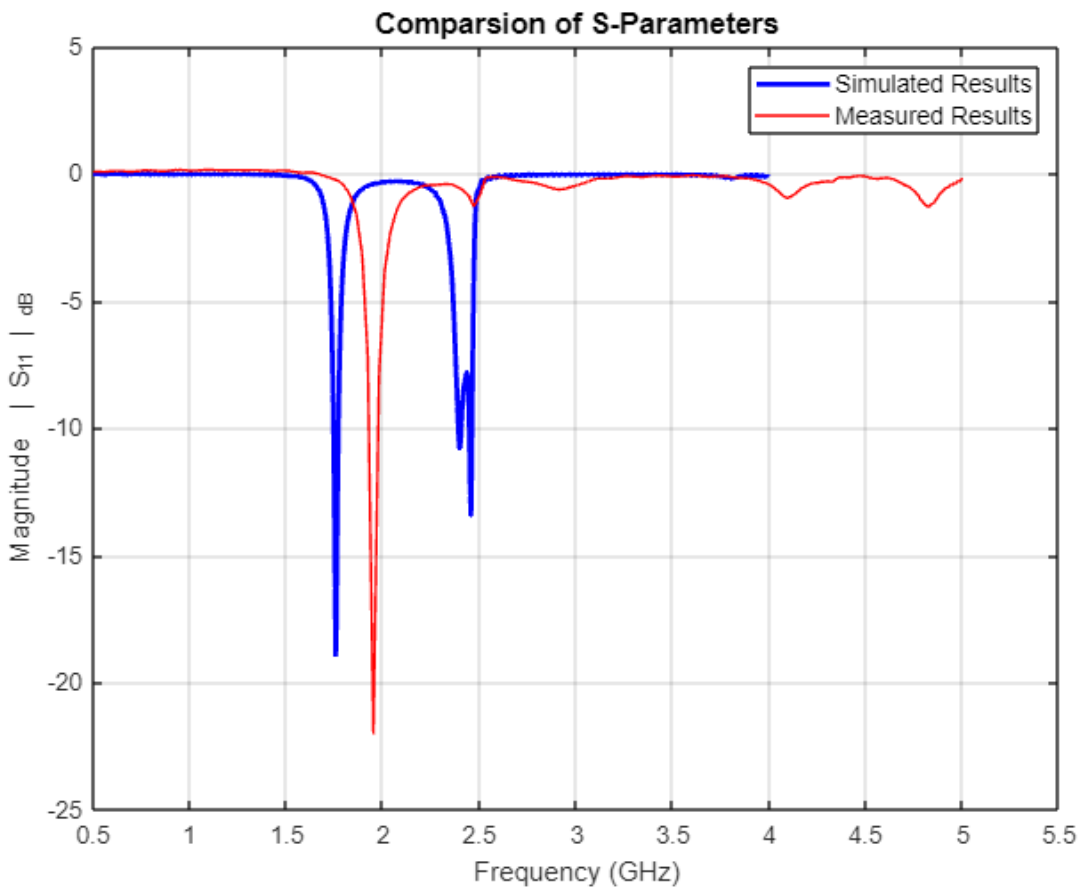


Figure 4.89 Simulated Vs. Measured Return Loss

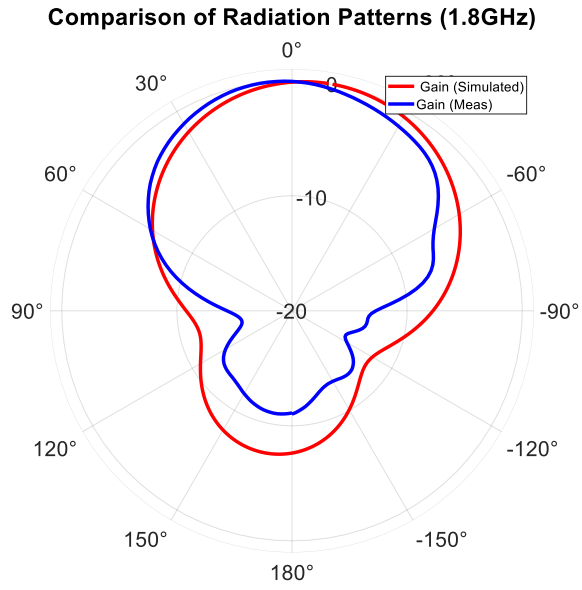


Figure 4.90 Simulated Vs. Measured Gain (1.8GHz)

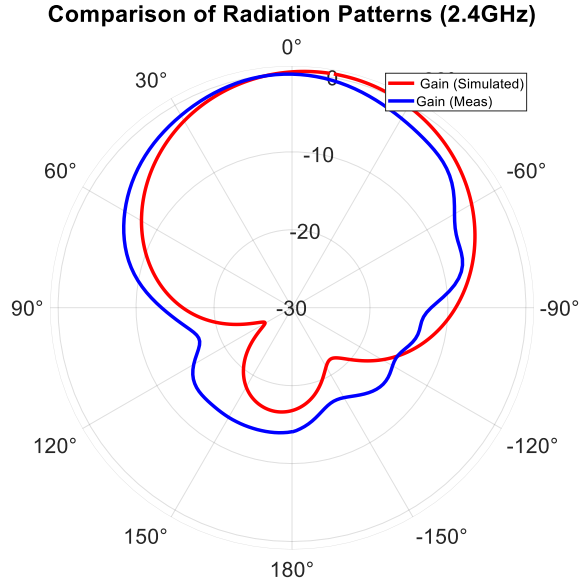


Figure 4.91 Simulated Vs. Measured Gain (2.45GHz)

Chapter # 5

Conclusion and Future Recommendations

5.1. Conclusion

A dual band circularly polarized stacked proximity coupled microstrip patch antenna is presented. This design has simple topology, frequency agility, flexibility with feed line and integration with MMIC. The design includes a cavity in the ground and a coax connection to the feed. The antenna gives two bands at 1.8GHz and 2.4GHz with the gain of 5.11 and 5.99dBi respectively. The antenna is circularly polarized and is of dimensions 54x54mm. It has a radiation efficiency of 90% and 75% at 1.8GHz and 2.4GHz respectively. The total efficiency is 85% and 70% at both these bands respectively. The compact size makes it suitable for RF energy harvesting applications. Here is a design comparison with state of the art results in a tabular form.

Reference	Year	Dielectric Material	Frequency (GHz)	Size Sq.mm	Bandwidth	Polarization	Cavity
[6]	2014	Rogers	X band	28	>30%	Dual	Yes
[5]	2010	Rogers	X-band	25	44%	None	Yes
[7]	2010	Rogers	X-band	500	27.6%	None	Yes
[16]	2017	Rogers	14.96	25	-	None	Yes
[15]	2011	Rogers	5.98-12.39	20	>70%	None	Yes
[8]	2023	FR-4, Rogers	2.4	60x80	27.7%	None	No
This Work	2023	Rogers	1.8-2.4	54x54	20%,80%	Yes	Yes

Table 3 Design comparison with state of the art

5.2. Future Recommendations

This thesis fulfills the requirement of an antenna design made for RF energy harvesting application targeting the GSM 1800 and Wi-Fi 2.4GHz bands respectively. However, improvisation of this design can further lead to improvement in bandwidth and more frequency bands at higher frequency ranges. A 3D cubicle model can also be made of this same design and a connection with rectifier can transform it to Rectenna for RF energy harvesting applications. Some of the few suggestions for future recommendations are given below:

- Increasing the bandwidth of the multilayered antenna.
- The design can perform efficiently by using a thicker version of the same substrate.
- Enhancement of the coupling between the substrate layers.
- A power combiner can be used to combine the antenna with rectifier.
- Rectenna can be made using the same antenna.

REFERENCES

- [1] Muhammad, A., Yaori, A.Y. and Kabir, A.M. (no date) Review of feeding techniques for microstrip patch antenna - ijcaonline.org. Available at: <https://www.ijcaonline.org/archives/volume178/number27/mohammed-2019-ijca-919010.pdf> (Accessed: 27 December 2023).
- [2] Yang, Q., Gu, J., Wang, D., Zhang, X., Tian, Z., Ouyang, C., ... & Zhang, W. (2014). Efficient flat metasurface lens for terahertz imaging. *Optics express*, 22(21), 25931-25939.
- [3] Katare, K. K., Biswas, A., & Akhtar, M. J. (2017). Microwave beam steering of planar antennas by hybrid phase gradient metasurface structure under spherical wave illumination. *Journal of Applied Physics*, 122(23), 234901.
- [4] Sun, H., Gu, C., Chen, X., Li, Z., Liu, L., & Martín, F. (2017). Ultra-wideband and broad-angle linear polarization conversion metasurface. *Journal of applied physics*, 121(17), 174902.
- [5] Khan, M. I., Fraz, Q., & Tahir, F. A. (2017). Ultra-wideband cross polarization conversion metasurface insensitive to incidence angle. *Journal of Applied Physics*, 121(4), 045103.
- [6] Ahmad, T., Rahim, A. A., Bilal, R. M. H., Noor, A., Maab, H., Naveed, M. A., ... & Saeed, M. A. (2022). Ultrawideband Cross-Polarization Converter Using Anisotropic Reflective Metasurface. *Electronics*, 11(3), 487.
- [7] Yang, X., Ding, Z., & Zhang, Z. (2021). Broadband linear polarization conversion across complete Ku band based on ultrathin metasurface. *AEU-International Journal of Electronics and Communications*, 138, 153884.
- [8] Tamoor, T., Shoaib, N., Ahmed, F., Hassan, T., Quddious, A., Nikolaou, S., ... & Abbasi, Q. H. (2021). A multifunctional ultrathin flexible bianisotropic metasurface with miniaturized cell size. *Scientific Reports*, 11(1), 1-14.
- [9] Lee, G. Y., Sung, J., & Lee, B. (2019). Recent advances in metasurface hologram technologies. *ETRI Journal*, 41(1), 10-22.
- [10] Bai, H., Wang, G. M., & Zou, X. J. (2020). A wideband and multi-mode metasurface antenna with gain enhancement. *AEU-International Journal of Electronics and Communications*, 126, 153402.
- [11] Wang, J., Yang, R., Ma, R., Tian, J., & Zhang, W. (2020). Reconfigurable multifunctional metasurface for broadband polarization conversion and perfect absorption. *IEEE Access*, 8, 105815-105823.
- [12] Dutta, R., Mitra, D., & Ghosh, J. (2020). Dual-band multifunctional metasurface for absorption and polarization conversion. *International Journal of RF and Microwave Computer-Aided Engineering*, 30(7), e22200.
- [13] Murugesan, A., Selvan, K., Iyer, A., Srivastava, K. V., & Alphones, A. (2021). A Review of Metasurface-Assisted RCS Reduction Techniques. *Progress In Electromagnetics Research B*, 94, 75-103.

- [14] C. Song et al., "Matching Network Elimination in Broadband Rectennas for High-Efficiency Wireless Power Transfer and Energy Harvesting," in *IEEE Transactions on Industrial Electronics*, vol. 64, no. 5, pp. 3950-3961, May 2017, doi: 10.1109/TIE.2016.2645505..
- [15] C. Song, Y. Huang, P. Carter, J. Zhou, S. D. Joseph and G. Li, "Novel Compact and Broadband Frequency-Selectable Rectennas for a Wide Input-Power and Load Impedance Range," in *IEEE Transactions on Antennas and Propagation*, vol. 66, no. 7, pp. 3306-3316, July 2018, doi: 10.1109/TAP.2018.2826568.
- [16] Fatima Khalid, Warda Saeed, Noshawan Shoaib, Muhammad U. Khan, Hammad M. Cheema, "Quad-Band 3D Rectenna Array for Ambient RF Energy Harvesting", *International Journal of Antennas and Propagation*, vol. 2020, Article ID 7169846, 23 pages, 2020. <https://doi.org/10.1155/2020/7169846>.
- [17] Ahmed, F., Hassan, T., & Shoaib, N. (2020). A multiband bianisotropic FSS with polarization-insensitive and angularly stable properties. *IEEE Antennas and Wireless Propagation Letters*, 19(10), 1833-1837.
- [18] Charola, S., Patel, S. K., Parmar, J., & Jadeja, R. (2022). Multiband Jerusalem cross-shaped angle insensitive metasurface absorber for X-band application. *Journal of Electromagnetic Waves and Applications*, 36(2), 180-192.
- [19] Gao, X., Yang, W. L., Ma, H. F., Cheng, Q., Yu, X. H., & Cui, T. J. (2018). A reconfigurable broadband polarization converter based on an active metasurface. *IEEE Transactions on Antennas and Propagation*, 66(11), 6086-6095.
- [20] M. Kumar, S. Kumar, A. S. Bhadauria and A. Sharma, "A Planar Integrated Rectenna Array With 3-D-Spherical DC Coverage for Orientation-Tolerant Wireless-Power-Transfer-Enabled IoT Sensor Nodes," in *IEEE Transactions on Antennas and Propagation*, vol. 71, no. 2, pp. 1285-1294, Feb. 2023, doi: 10.1109/TAP.2022.3228708.
- [21] D. Sun and L. You, "A Broadband Impedance Matching Method for Proximity-Coupled Microstrip Antenna," in *IEEE Transactions on Antennas and Propagation*, vol. 58, no. 4, pp. 1392-1397, April 2010, doi: 10.1109/TAP.2010.2041312.
- [22] S. Chen, Y. Liu, Y. Ren and Q. H. Liu, "A broadband dual-polarized microstrip antenna with cavity-backed proximity-coupling feeding," 2014 XXXIth URSI General Assembly and Scientific Symposium (URSI GASS), Beijing, China, 2014, pp. 1-3, doi: 10.1109/URSIGASS.2014.6929080.
- [23] D. Sun, W. Dou and L. You, "Application of Novel Cavity-Backed Proximity-Coupled Microstrip Patch Antenna to Design Broadband Conformal Phased Array," in *IEEE Antennas and Wireless Propagation Letters*, vol. 9, pp. 1010-1013, 2010, doi: 10.1109/LAWP.2010.2089490.
- [24] S. S. Sruthi, I. S. Rao and M. D. Rao, "Design of a dual-polarized antenna using square backed cavity," 2017 International Conference on Innovations in Information, Embedded and Communication Systems (ICIIECS), Coimbatore, India, 2017, pp. 1-4, doi: 10.1109/ICIIECS.2017.8276087..
- [25] Yu, Y., Xiao, F., He, C., Jin, R., & Zhu, W. (2020). Double-arrow metasurface for dual-band and dual-mode polarization conversion. *Optics express*, 28(8), 11797-11805.

- [26] Dutta, R., Ghosh, J., Yang, Z., & Zhang, X. (2021). Multi-Band Multi-Functional Metasurface-Based Reflective Polarization
- [27] Bokhari, S. H. A., & Cheema, H. M. (2020). A bilayered, broadband, angularly robust chiral metasurface for asymmetric transmission. *IEEE Antennas and Wireless Propagation Letters*, 20(1), 23-27.
- [28] Bokhari, S. H. A., & Cheema, H. M. (2020). Broadband asymmetric transmission via angle-induced chirality enhancement in split ring resonators. *Journal of Applied Physics*, 128(6), 063102.
- [29] Huang, X., Yang, D., Yu, S., Guo, L., Guo, L., & Yang, H. (2014). Dual-band asymmetric transmission of linearly polarized wave using Π -shaped metamaterial. *Applied Physics B*, 117(2), 633-638.
- [30] Kossifos, K. M., Antoniadis, M. A., & Georgiou, J. (2020). Integrated-circuit enabled adaptive metasurface absorber with independent tuning of orthogonal polarization planes. *IEEE Access*, 8, 50227-50235.
- [31] Ahmad, Noman & Aslam, Javaria & Nawaz, Haq & Shahid, Humayun & Shoaib, Noshawan. (2021). Dual circularly polarized series-fed patch antenna array integrated with beam switching network. *International Journal of Numerical Modeling: Electronic Networks, Devices and Fields*. 34. 10.1002/jnm.2885.

APPENDIX A

Abbreviations & Acronyms

RHCP	Right hand circularly polarized
LHCP	Left hand circularly polarized
GSM	Global system for mobile communication
Wi-Fi	Wireless Fidelity
RF	Radio Frequency
OCFD	Off center fed dipole
IoT	Internet of Things
WPT	Wireless Power Transfer
WEH	Wireless Energy Harvesting